Supplementary Information for

# Direct regeneration of degraded lithium-ion battery cathodes with a multifunctional organic lithium salt

Guanjun Ji[1,2#], Junxiong Wang[1,2#], Zheng Liang[2*], Kai Jia[1,2], Jun Ma[1], Zhaofeng Zhuang[1], Guangmin Zhou[1*], Hui-Ming Cheng[3,4*]

[1] *Tsinghua-Berkeley Shenzhen Institute & Tsinghua Shenzhen International Graduate School, Tsinghua University, Shenzhen 518055, China*

[2] *Frontiers Science Center for Transformative Molecules, School of Chemistry and Chemical Engineering, Shanghai Jiao Tong University, Shanghai 200240, China*

[3] *Faculty of Materials Science and Engineering / Institute of Technology for Carbon Neutrality, Shenzhen Institute of Advanced Technology, Chinese Academy of Science, Shenzhen 518055, China*

[4] *Shenyang National Laboratory for Materials Science, Institute of Metal Research, Chinese Academy of Sciences, Shenyang 110016, China*

* Corresponding authors: Zheng Liang (Email: liangzheng06@sjtu.edu.cn); Guangmin Zhou (Email: guangminzhou@sz.tsinghua.edu.cn); Hui-Ming Cheng (Email: cheng@imr.ac.cn)

# These authors contributed equally to this work.

**This file includes:**

Supplementary Text

Supplementary Fig. 1 to Fig. 30

Supplementary Table 1 to Table 19

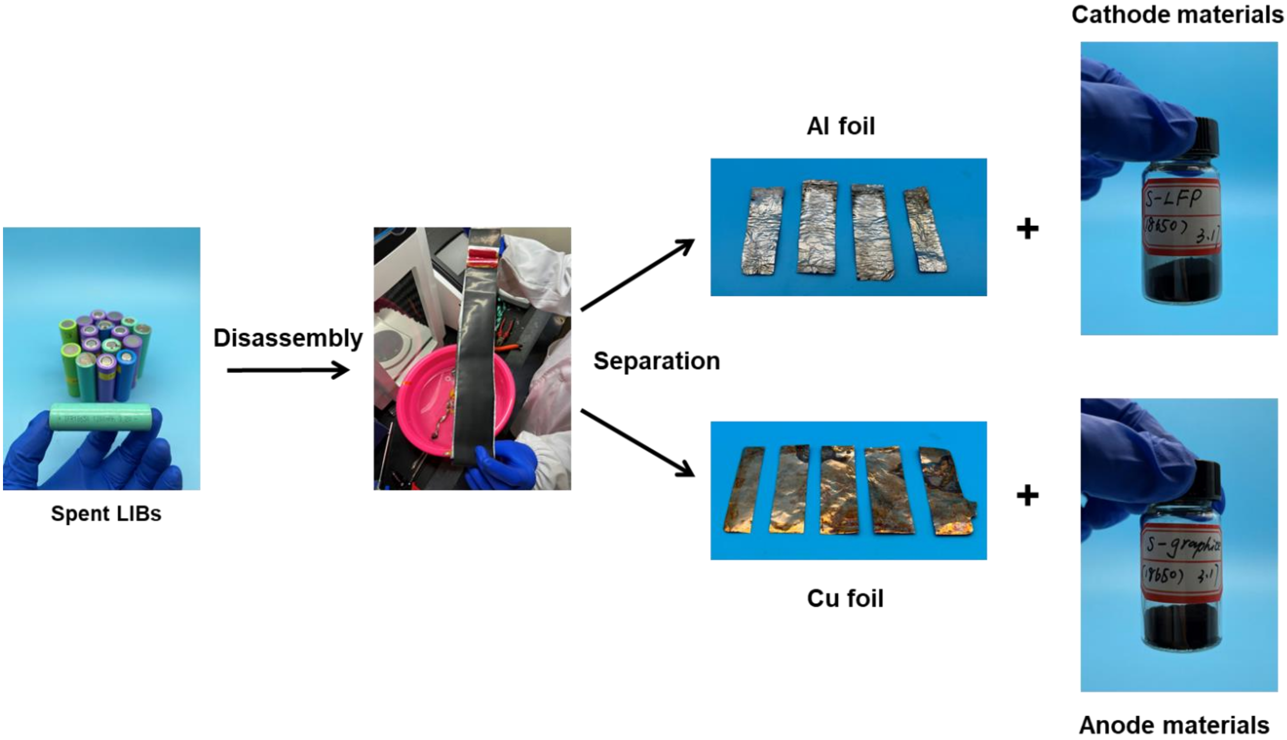


**Supplementary Fig. 1 Recycling procedure of spent LIBs.** 18650 degraded LIBs (1.2 Ah) were manually disassembled in a fume cupboard and the cathodes, anodes, and separators removed. The cathode sheets were immersed in water and the spent powder could then be easily separated from the Al foil due to its water-based binder. For the anode sheets, spent graphite powder was also collected during the same operation.

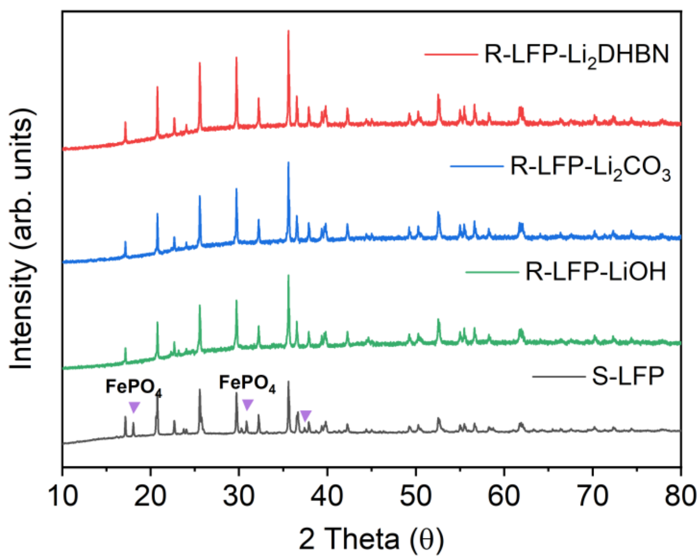


**Supplementary Fig. 2** XRD spectra of S-LFP, R-LFP-LiOH, R-LFP- $Li_2CO_3$, and R-LFP-$Li_2$DHBN.

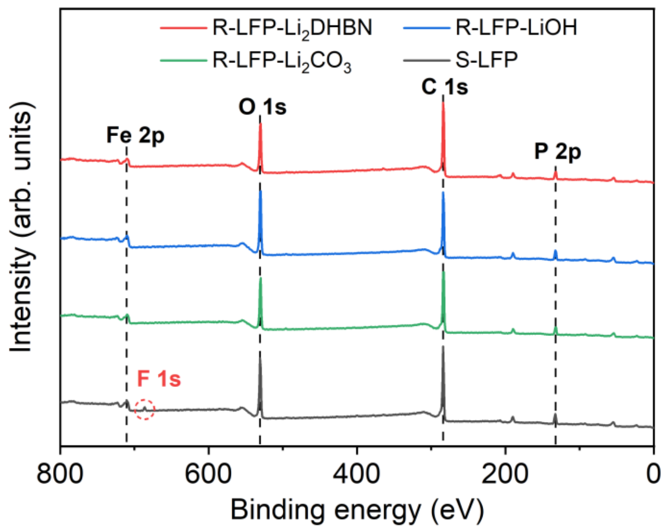


**Supplementary Fig. 3** XPS survey of S-LFP, R-LFP-LiOH, R-LFP-$Li_2CO_3$, and R-LFP-$Li_2$DHBN.

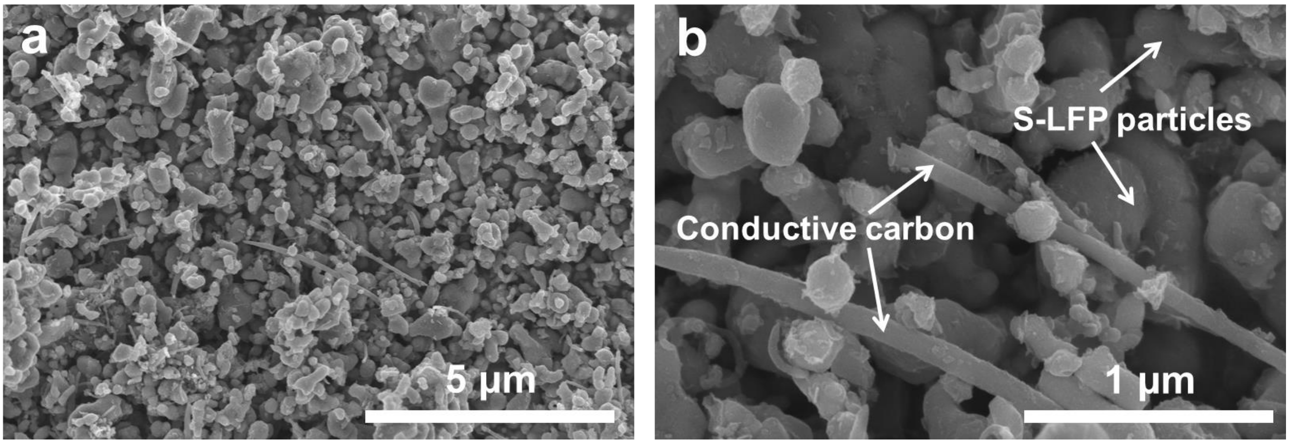


**Supplementary Fig. 4** SEM images of degraded LFP cathode materials at **a** low and **b** high resolutions.

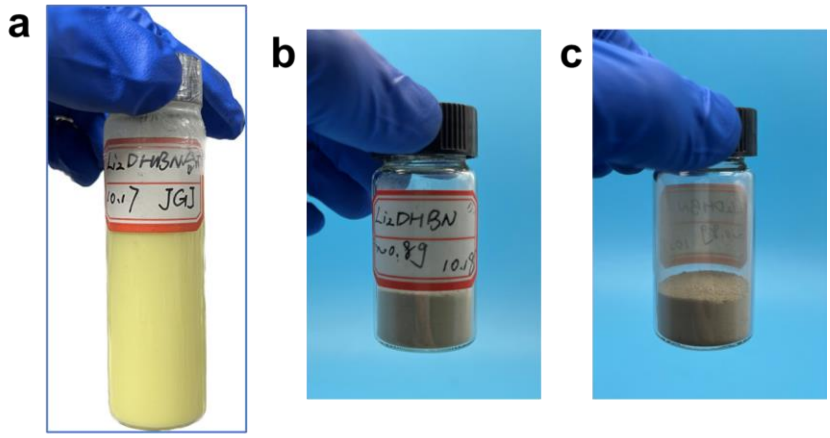


**Supplementary Fig. 5** The pictures during $Li_2$DHBN synthesis process. **a** A yellow solution before filtration. **b, c** The final $Li_2$DHBN precipitate after filtration and dry.

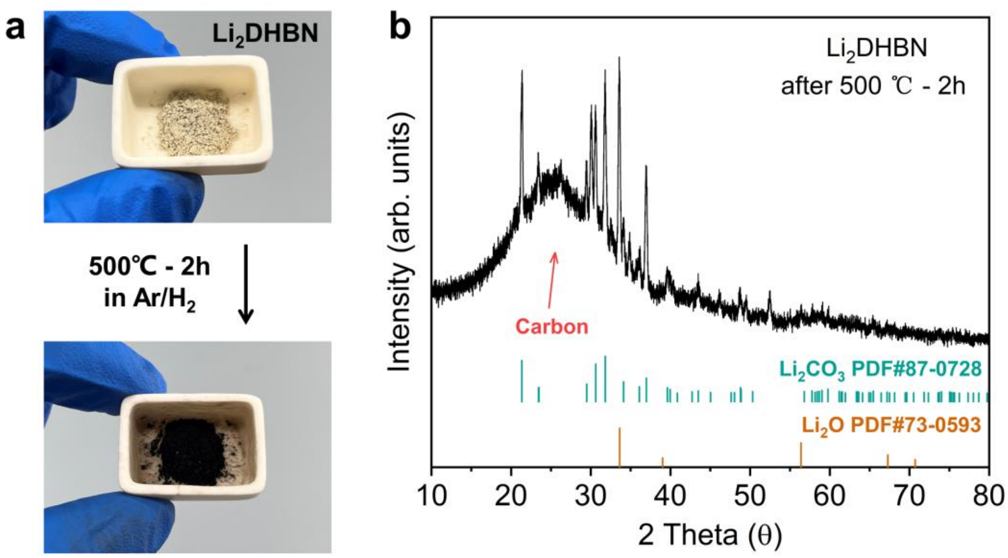


**Supplementary Fig. 6 a** The pictures of $Li_2$DHBN before and after heat treatment. **b** XRD spectra of $Li_2$DHBN after heat treatment.

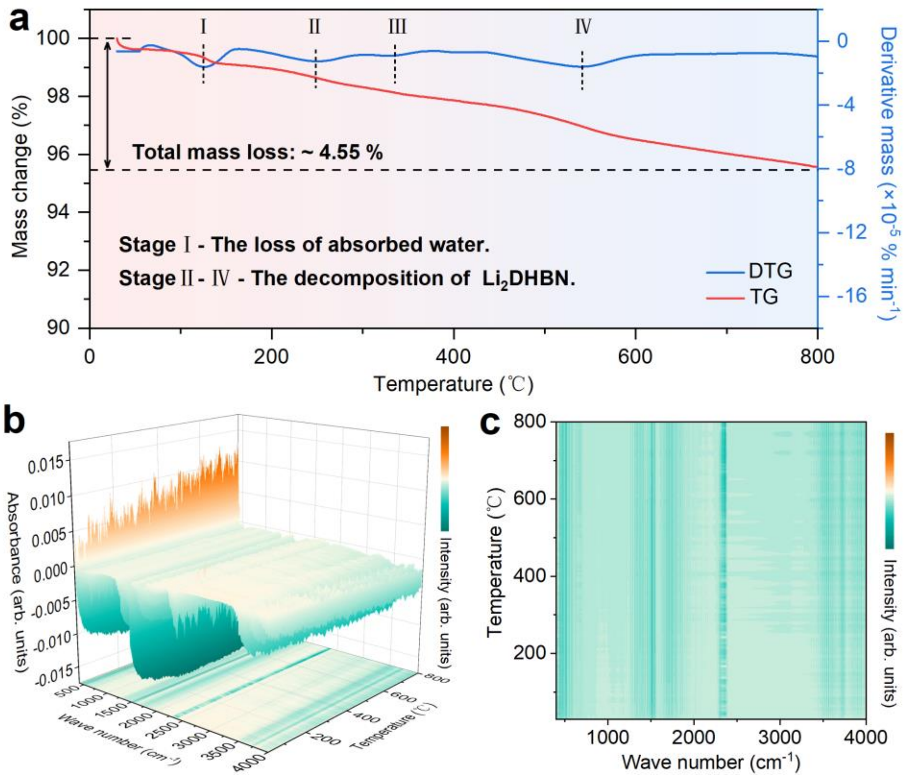


**Supplementary Fig. 7 a** TG-DTA, **b** TG-IR, and **c** IR contour map of the mixture of S-LFP powder and $Li_2$DHBN. To simulate our experimental process, the mixture of S-LFP powder and $Li_2$DHBN was also used for TR-FTIR measurements. The optimum weight of organic lithium salt is 5 wt%. The peaks are not obvious from the IR contour map due to the small quantity of $Li_2$DHBN. TG-DTA results show the same decomposition process as **Fig. 1e**.

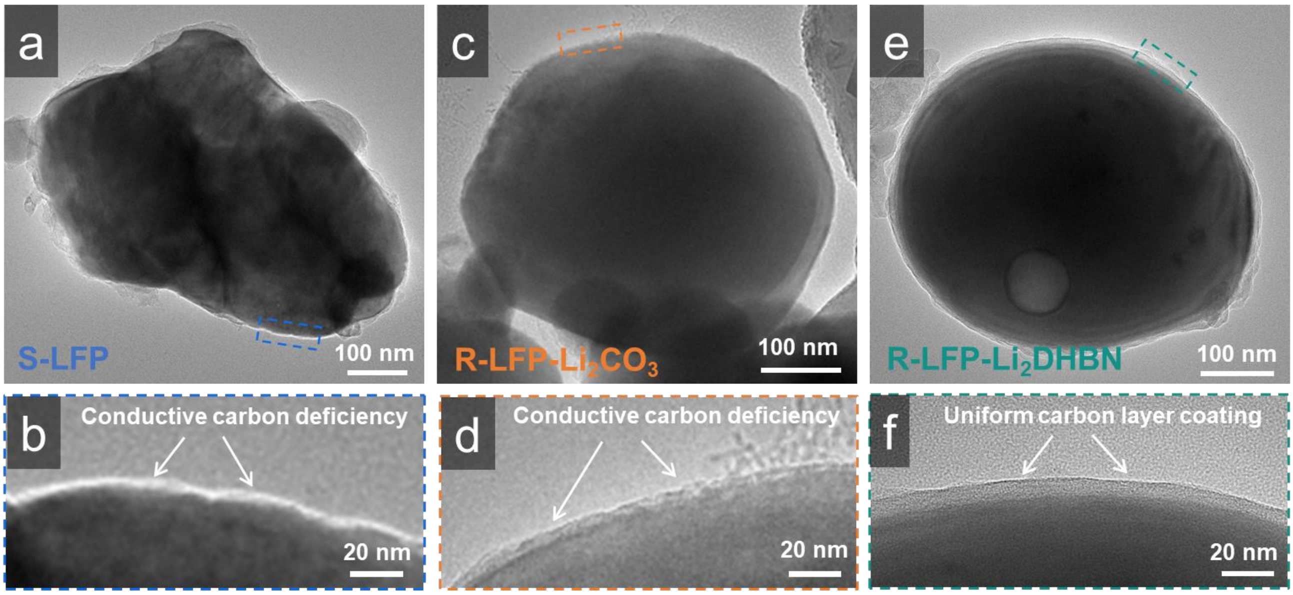


**Supplementary Fig. 8** TEM images and corresponding enlarged figures of **a, b** S-LFP, **c, d** R-LFP-$Li_2CO_3$, and **e, f** R-LFP-$Li_2DHBN$.

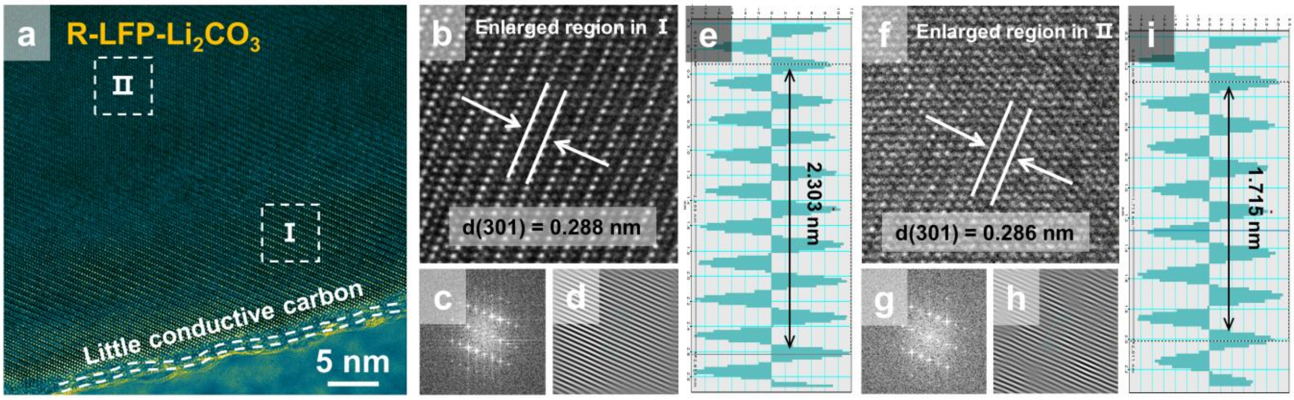


**Supplementary Fig. 9 Microstructure characterization of R-LFP-$Li_2CO_3$ cathode. a** TEM image, **b, f** enlarged figures, **c, g** SAED images from FFT results, **d, h** inverse FFT results, and **e, i** the corresponding line profiles in Supplementary Figs. 9d and 9h.

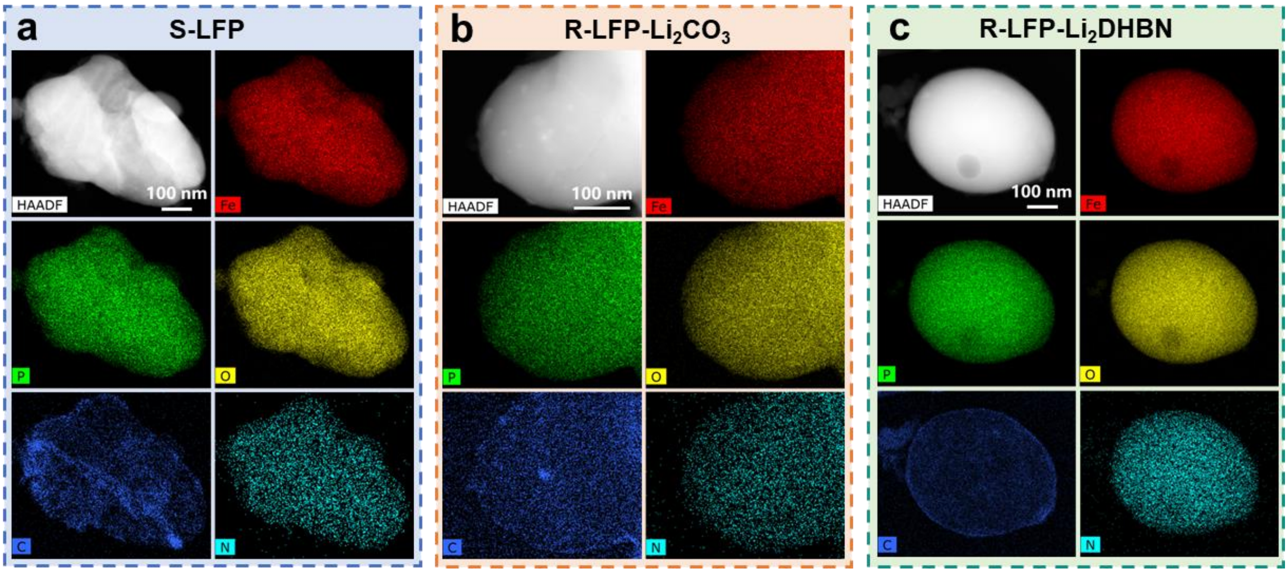


**Supplementary Fig. 10** EDS elemental maps of **a** S-LFP, **b** R-LFP-$Li_2CO_3$ and **c** R-LFP-$Li_2$DHBN.

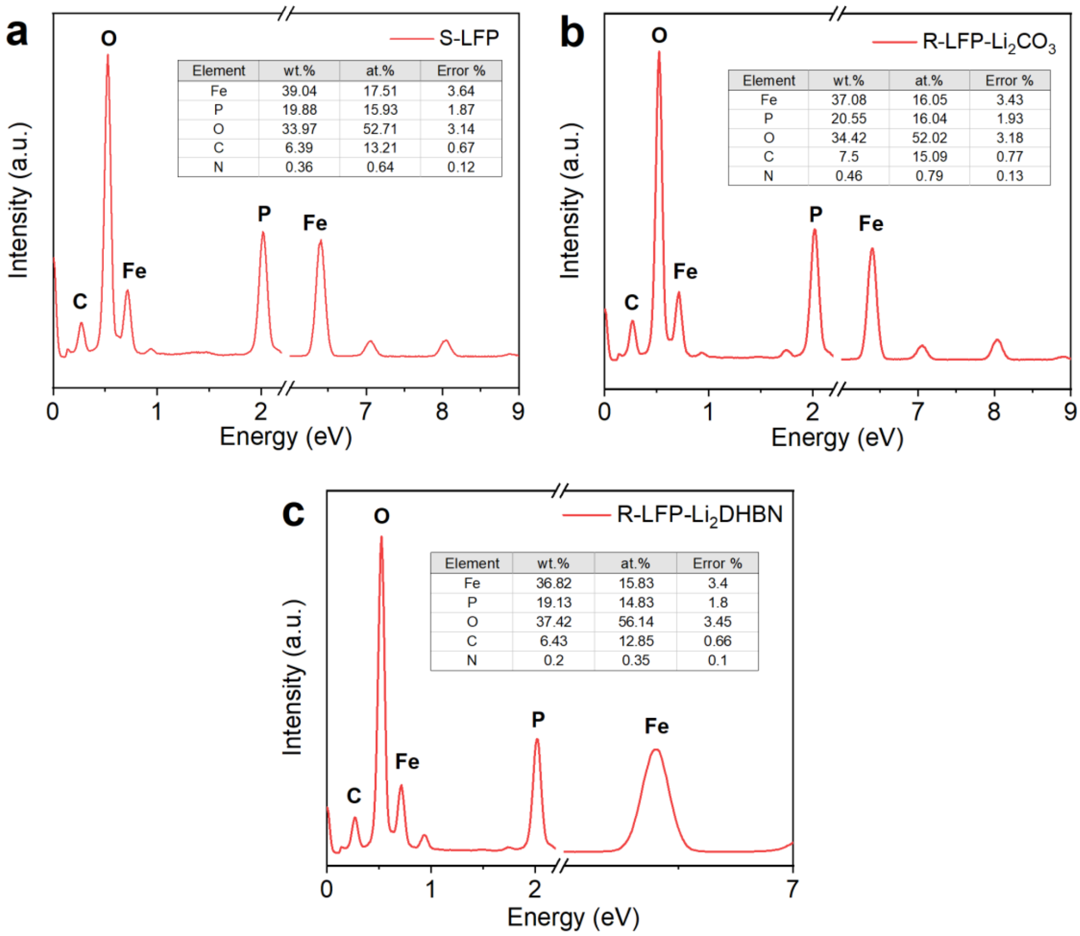


**Supplementary Fig. 11** EDS energy spectra of **a** S-LFP, **b** R-LFP-$Li_2CO_3$ and **c** R-LFP-$Li_2$DHBN.

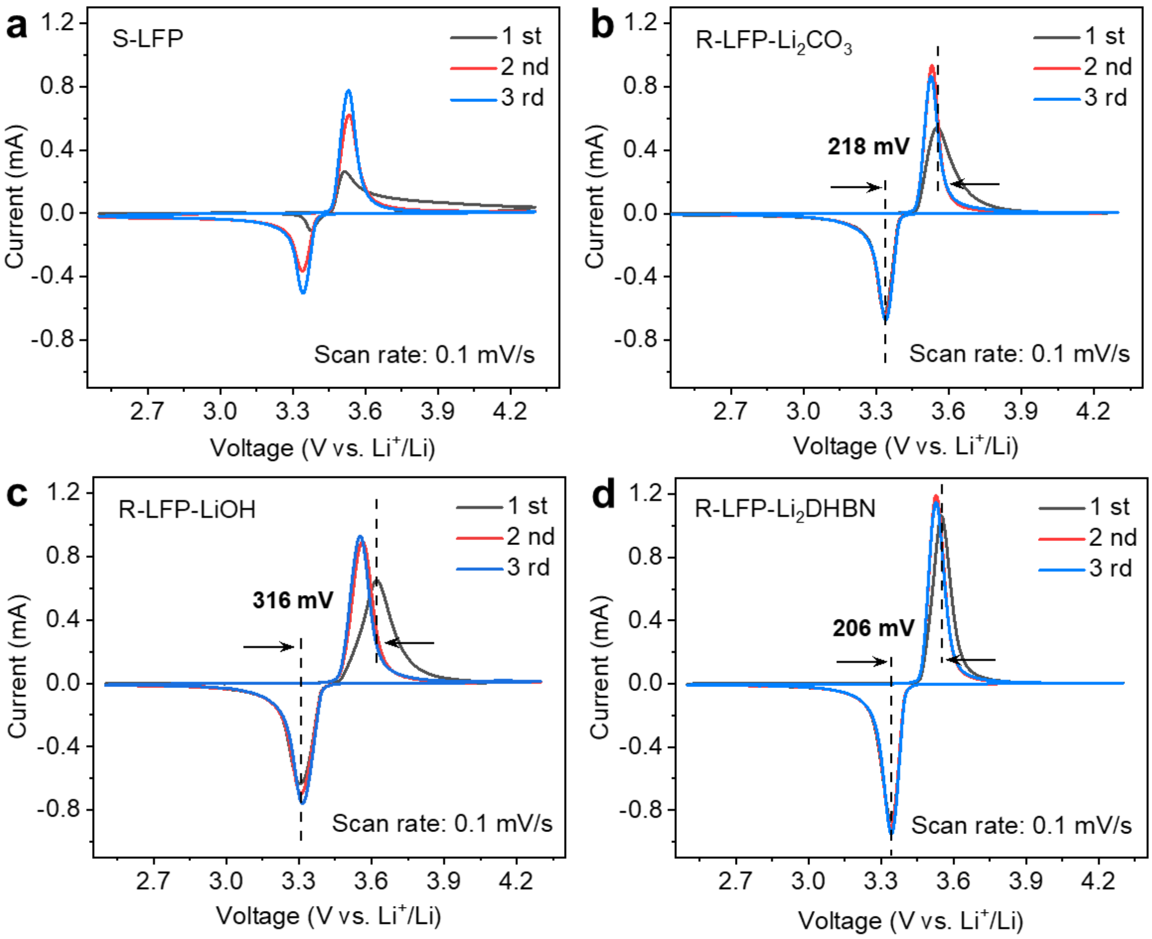


**Supplementary Fig. 12** The initial three CV curves of **a** S-LFP, **b** R-LFP-LiOH, **c** R-LFP-$Li_2CO_3$, **d** R-LFP-$Li_2$DHBN.

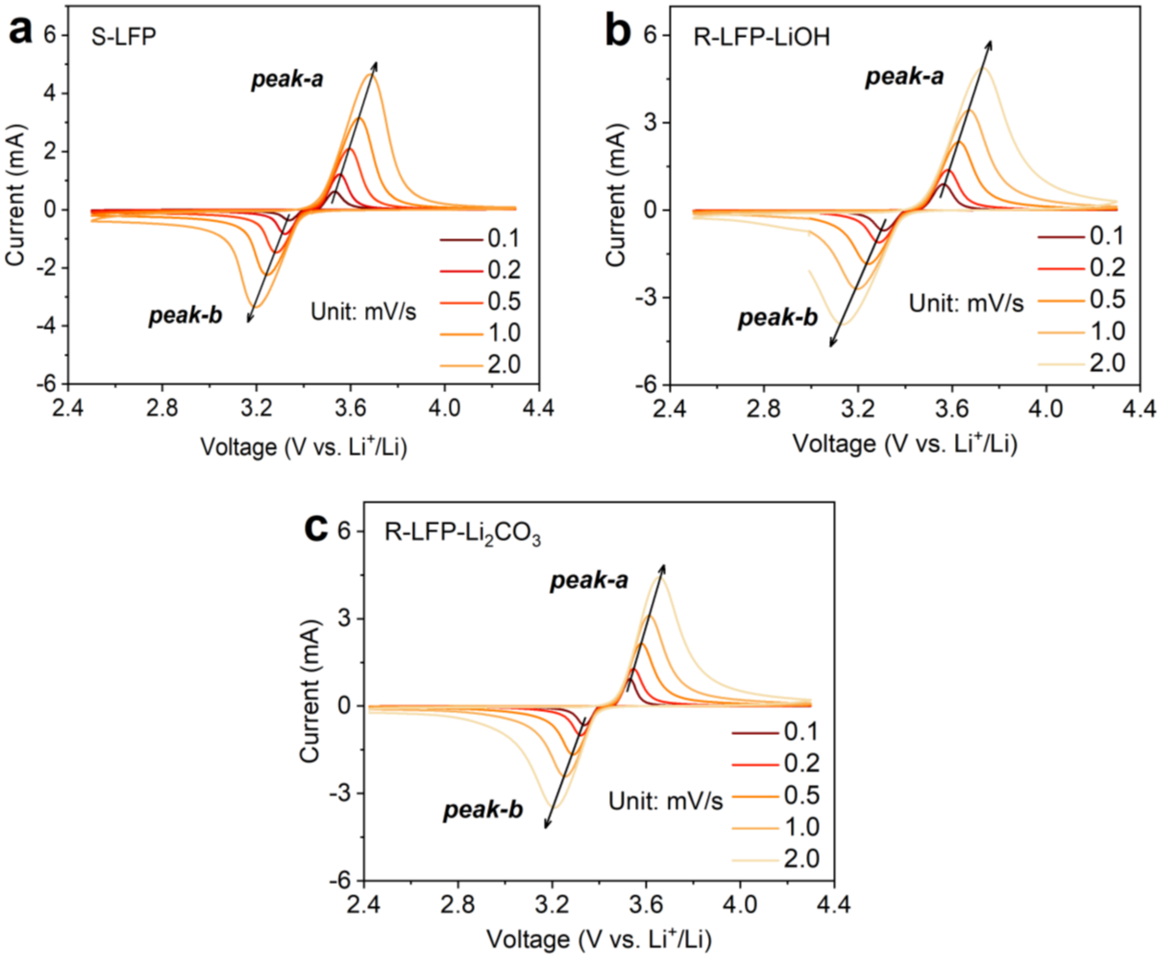


**Supplementary Fig. 13** CV curves at different scan rates of **a** S-LFP, **b** R-LFP-LiOH, and **c** R-LFP-$Li_2CO_3$.

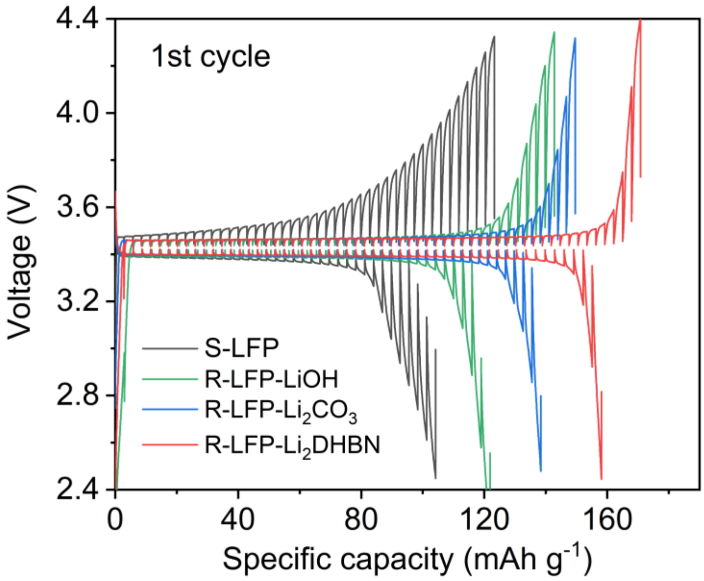


**Supplementary Fig. 14** GITT curves during the first cycle of S-LFP, R-LFP-LiOH, R-LFP- $Li_2CO_3$, and R-LFP-$Li_2$DHBN.

The Li-ion diffusion rate calculated from the GITT curve is based on the following formula according to Fick's second law of diffusion[1, 2, 3]:

$$D=4/\pi\tau\ (n_M V_M/S)^2(\Delta E_S/\Delta E_t)^2$$

where τ is the duration of the current pulse, $n_M$ is the number of moles, $V_M$ is the molar volume of the electrode, $S$ is the electrode-electrolyte contact area, and $\Delta E_S$ and $\Delta E_t$ are the changes in the steady state potential and the total change during the current flux by deducting the IR drop, respectively. In our experiments, $\tau = 1800$ s, $n_M = m/M_{LFP}$, $M_{LFP} = 157.76$ g mol$^{-1}$, $V_M = 20.5$ cm$^3$ mol$^{-1}$, $S = 1.13$ cm$^3$.

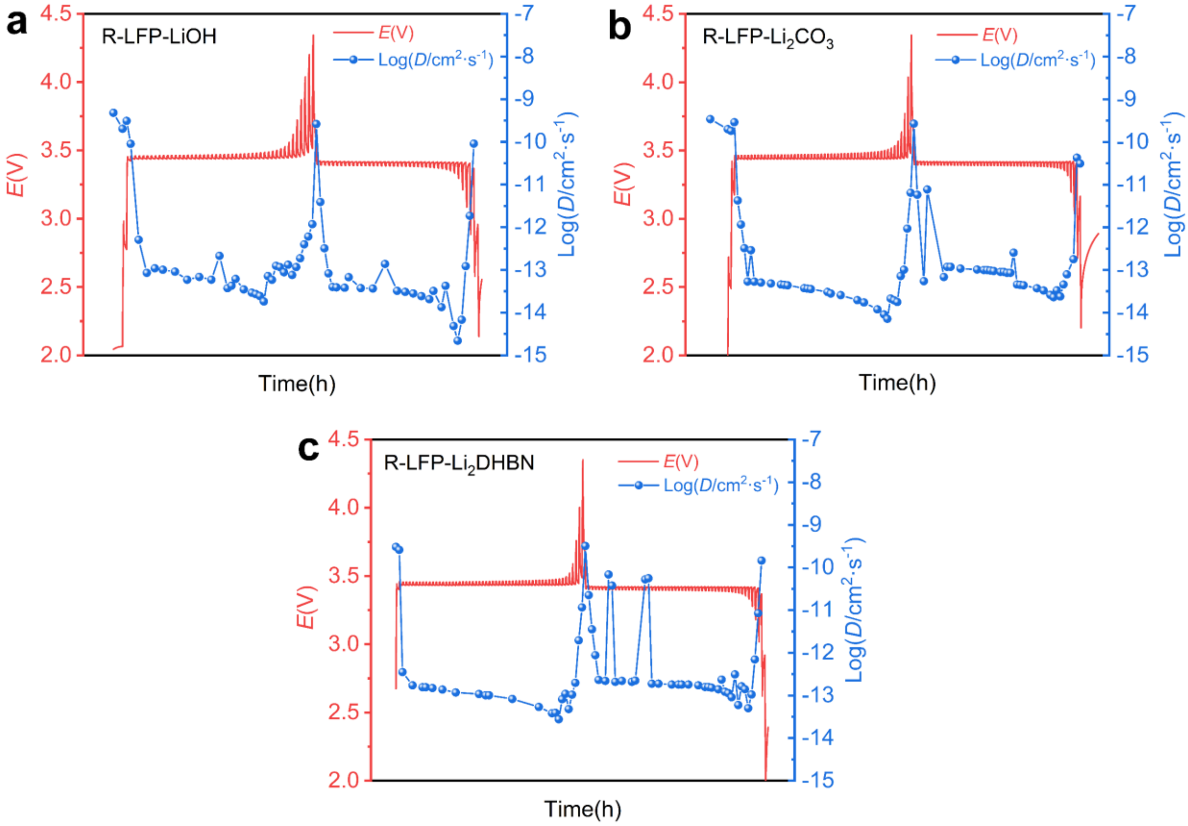


**Supplementary Fig. 15** GITT profiles for the discharge/charge process (red curves) and diffusion coefficients (blue curves) of **a** R-LFP-LiOH, **b** R-LFP- $Li_2CO_3$, and **c** R-LFP-$Li_2$DHBN.

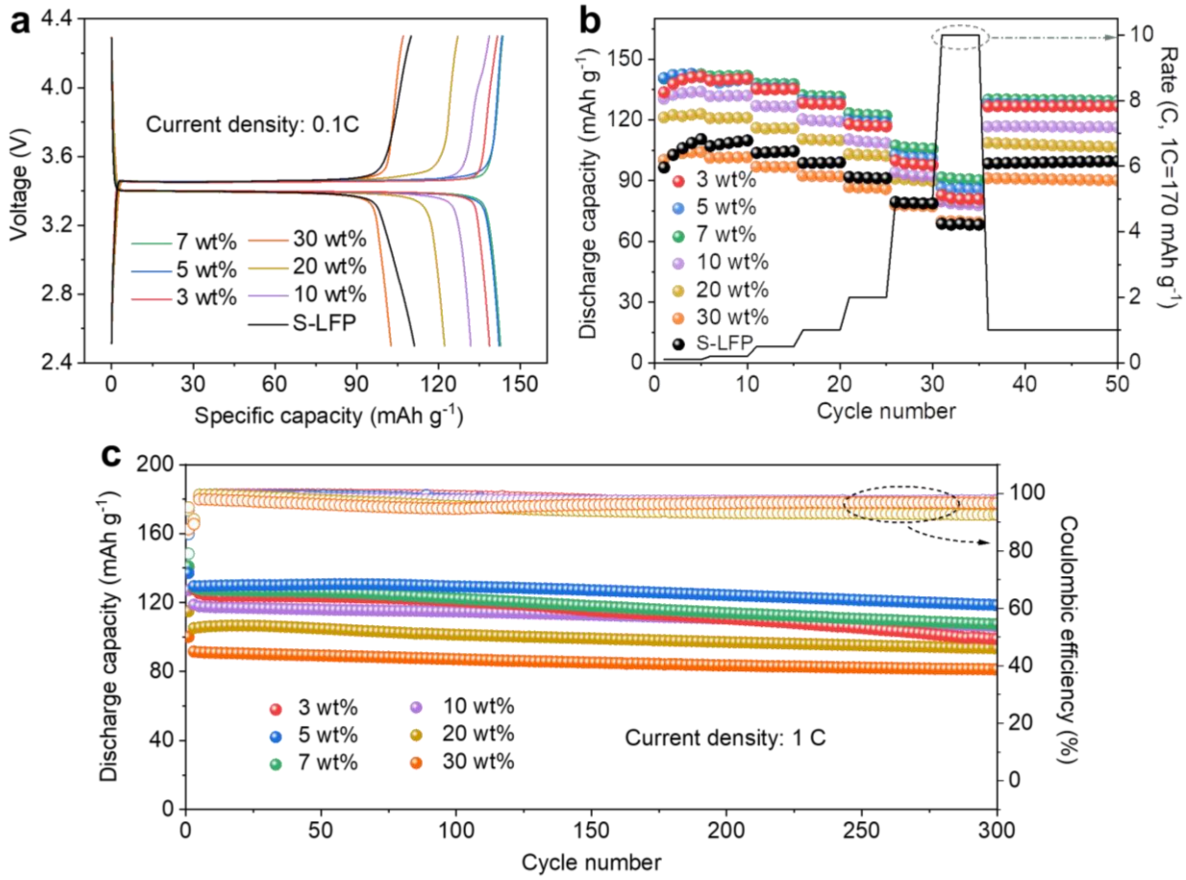


**Supplementary Fig. 16** The electrochemical performance obtained from different usages of $Li_2DHBN$. **a** Charge-discharge curves, **b** rate capabilities, **c** cycling performance of R-LFP-$Li_2DHBN$.

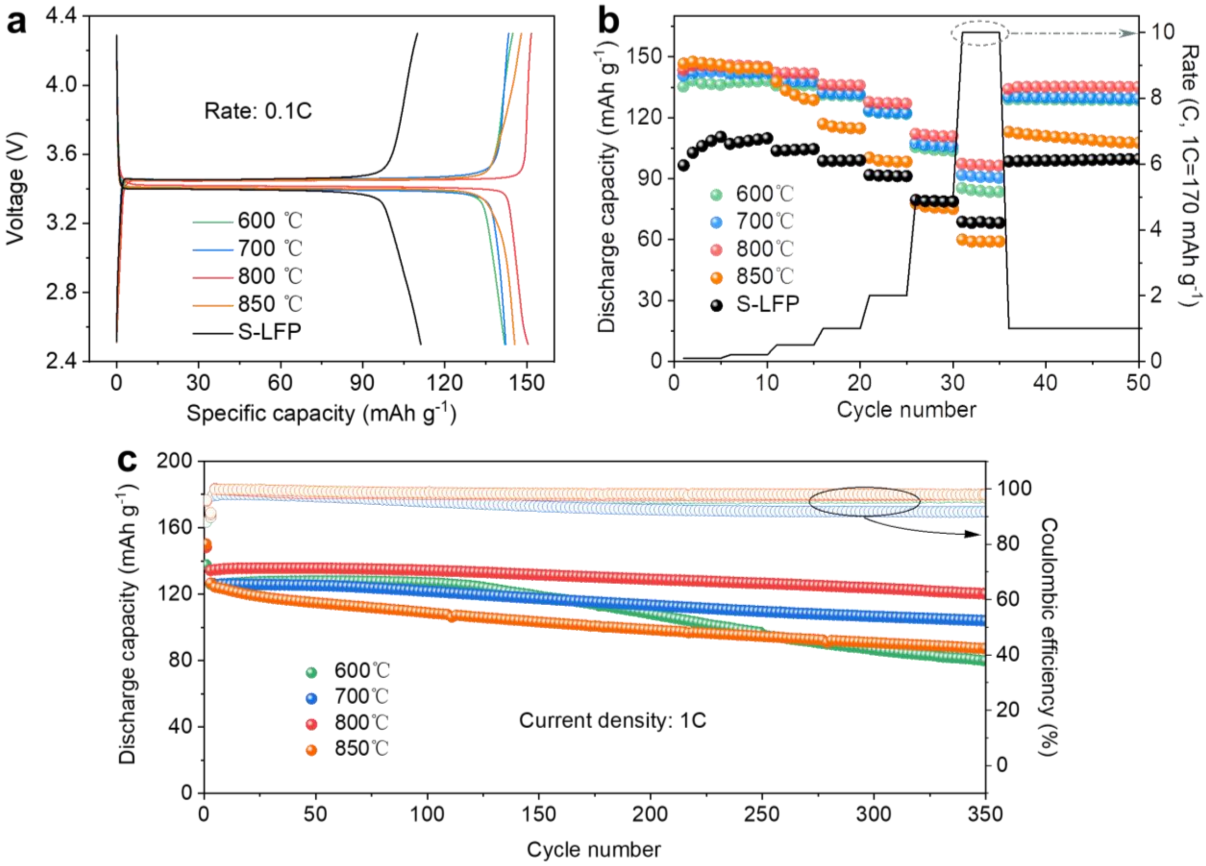


**Supplementary Fig. 17** The electrochemical performance obtained at different temperatures. **a** Charge-discharge curves, **b** rate capabilities, **c** cycling performance of R-LFP-$Li_2$DHBN.

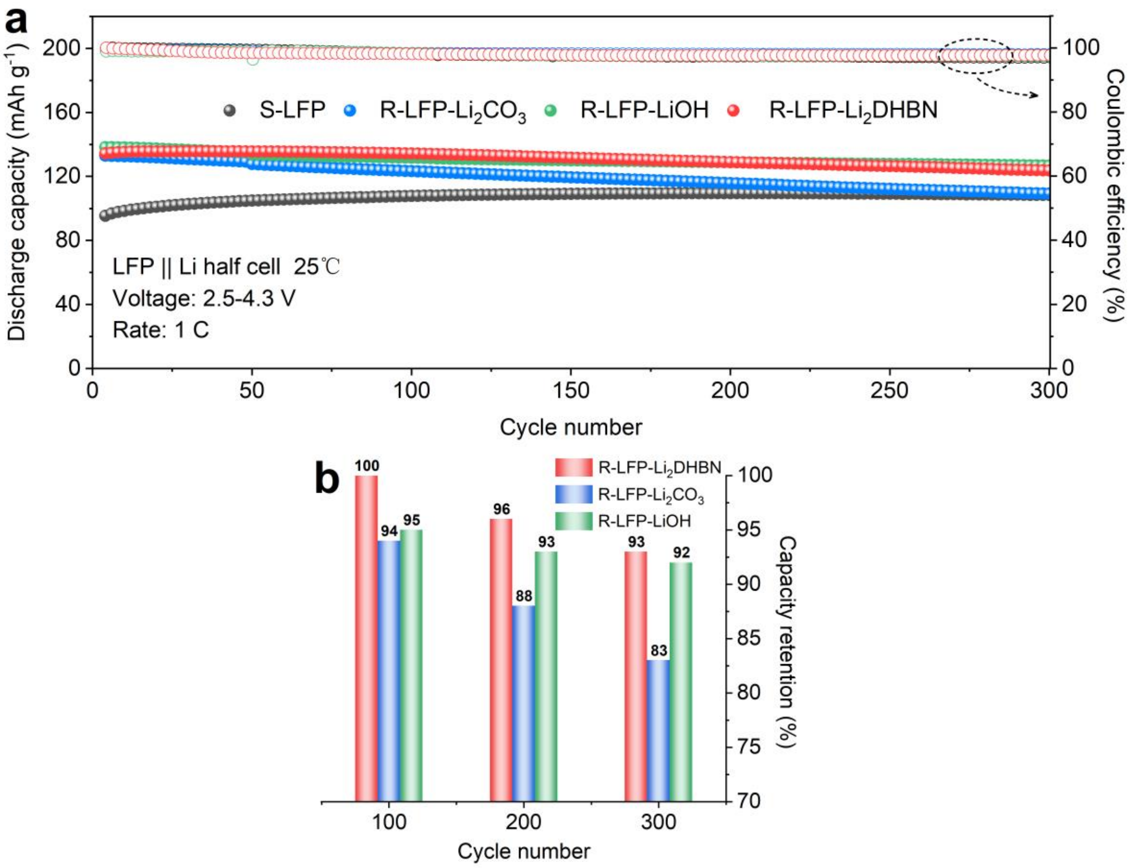


**Supplementary Fig. 18 a** The cycling performance at 1 C rate and **b** the corresponding capacity retentions of S-LFP, R-LFP-LiOH, R-LFP- $Li_2CO_3$, and R-LFP-$Li_2$DHBN.

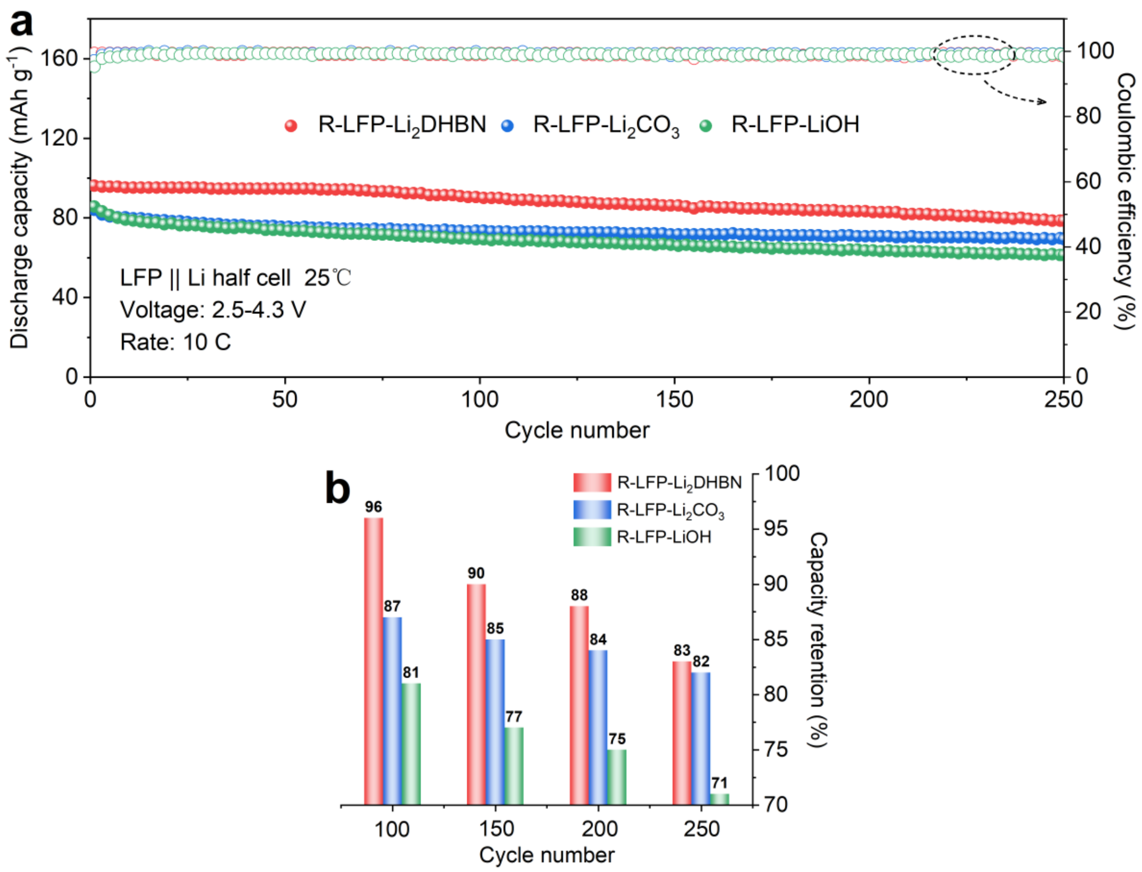


**Supplementary Fig. 19 a** The cycling performance at 10 C rate and **b** the corresponding capacity retentions of R-LFP-LiOH, R-LFP- $Li_2CO_3$, and R-LFP-$Li_2$DHBN.

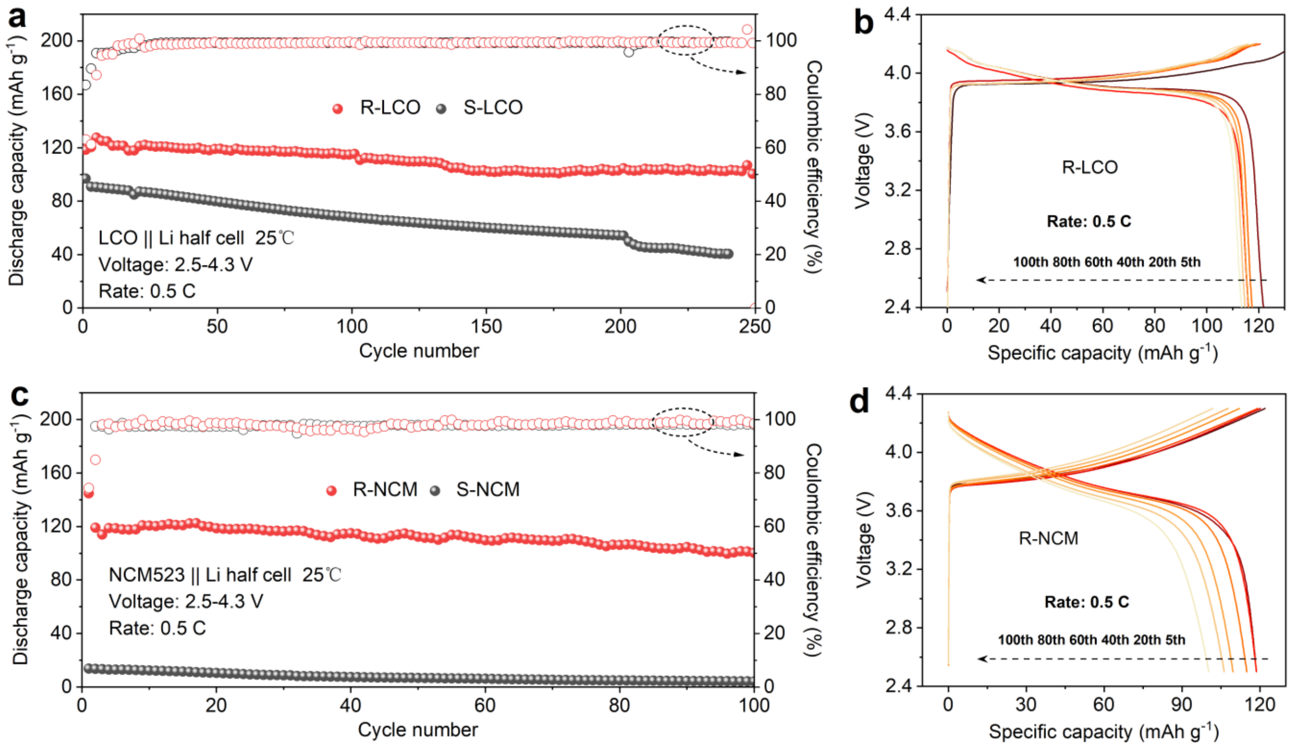


**Supplementary Fig. 20 Demonstration of the versatility of $Li_2$DHBN.** The cycling performance and charge-discharge profiles at a rate of 0.5 C of **a, b** R-NCM and **c, d** R-LCO.

To demonstrate the versatility of the organic lithium salt, S-LCO and S-NCM cathodes were also investigated under the optimal experimental conditions. As depicted in **Supplementary Fig. 20**, the R-LCO sample has a specific discharge capacity of 125 mAh $g^{-1}$ after 250 cycles with a high retention of 83%. In comparison, the S-LCO could only retain a capacity of 90 mAh $g^{-1}$ which decreased sharply after 200 cycles. For the R-NCM sample, the improved specific capacity reached about 120 mAh $g^{-1}$ and retained 84% of the initial value. The original S-NCM sample was almost completely degraded after long cycling. It is concluded that the $Li_2$DHBN can be used to restore different types of spent LIB cathodes with different degrees of degradation, thus providing a competitive lithium supplement for future direct regeneration technology.

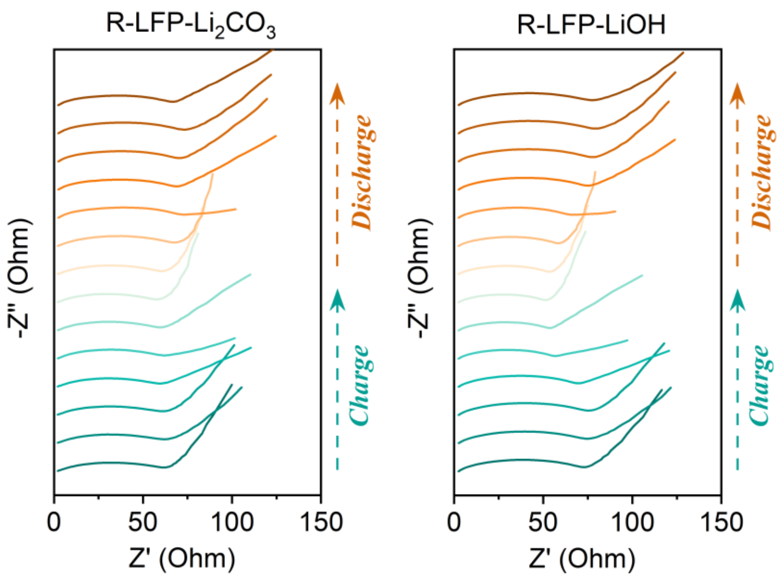


**Supplementary Fig. 21** The impedance spectra of **a** R-LFP-$Li_2CO_3$ and **b** R-LFP-LiOH collected during the first cycle.

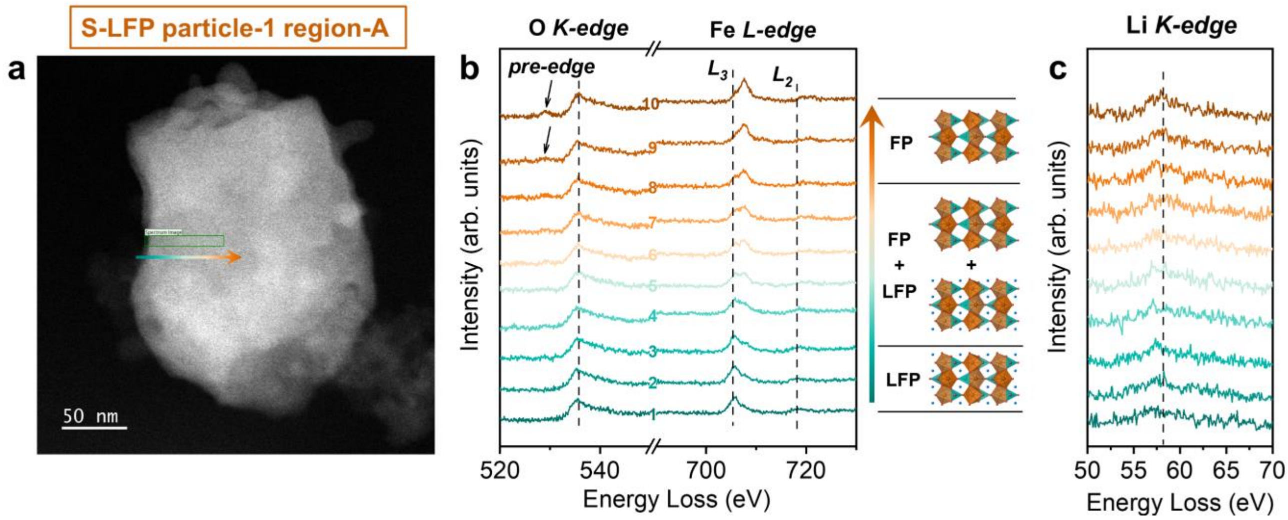


**Supplementary Fig. 22 a** STEM image, **b** O K-edge and Fe L-edge, and **c** Li K-edge EELS of S-LFP particle-1.

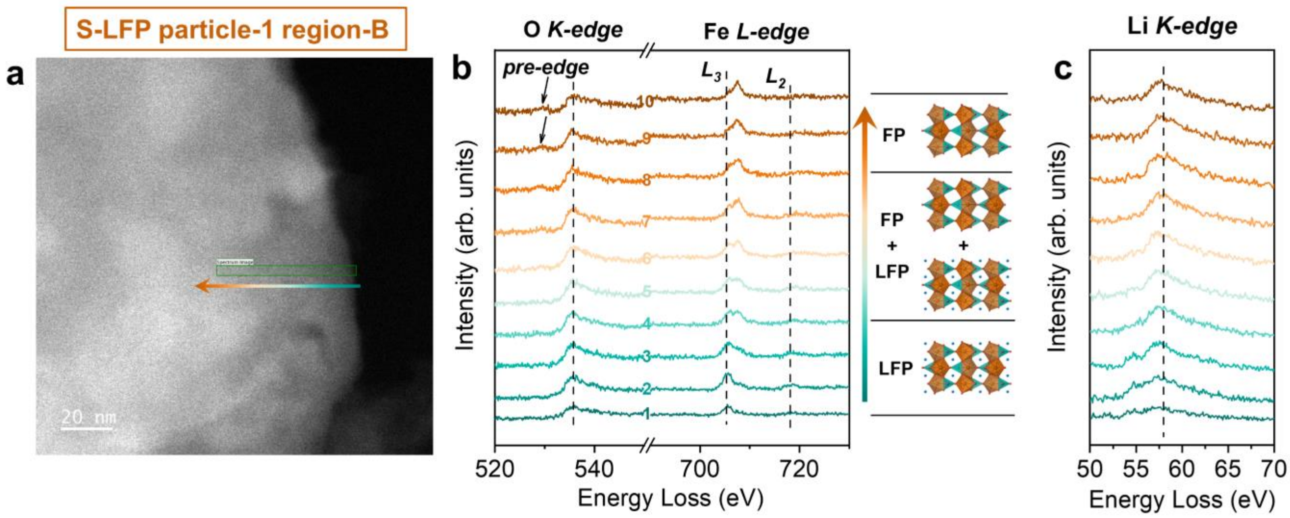


**Supplementary Fig. 23 a** STEM image, **b** O K-edge and Fe L-edge, and **c** Li K-edge EELS of S-LFP particle-1.

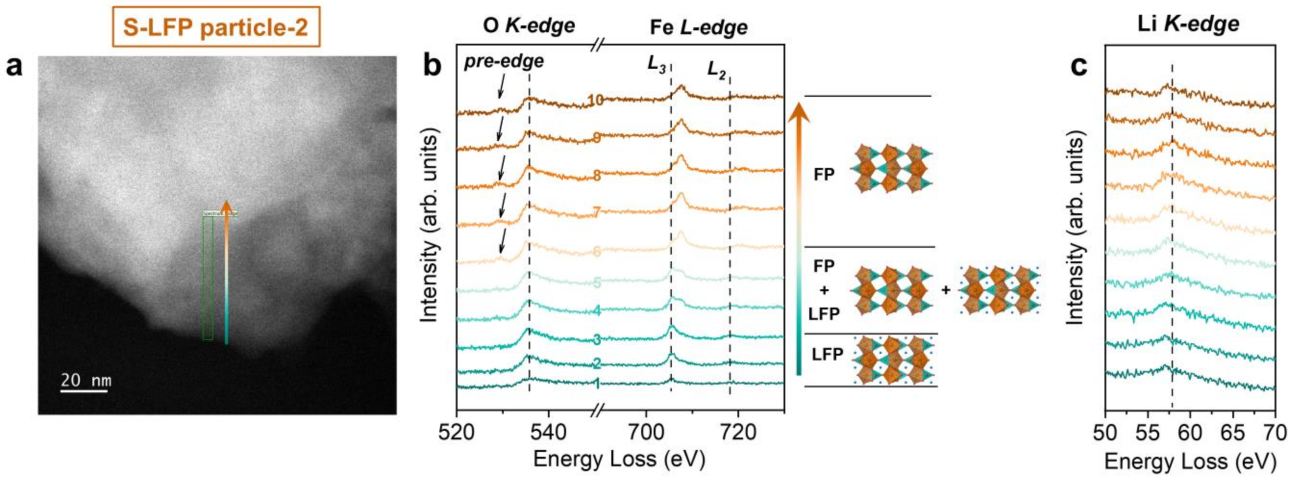


**Supplementary Fig. 24** **a** STEM image, **b** O K-edge and Fe L-edge, and **c** Li K-edge EELS of S-LFP particle-2.

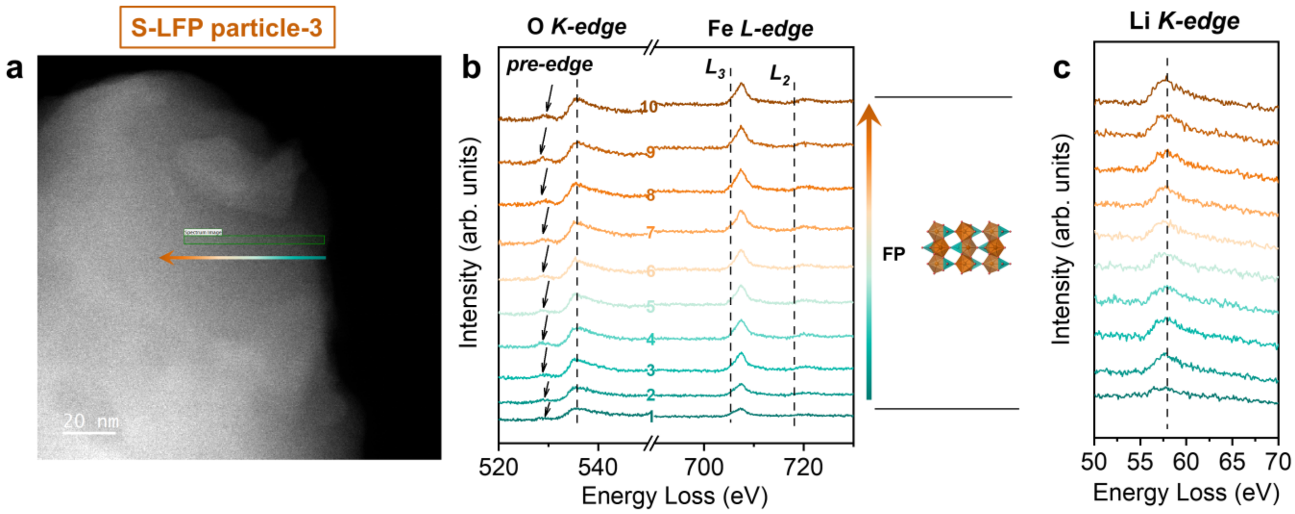


**Supplementary Fig. 25** **a** STEM image, **b** O K-edge and Fe L-edge, and **c** Li K-edge EELS of S-LFP particle-3.

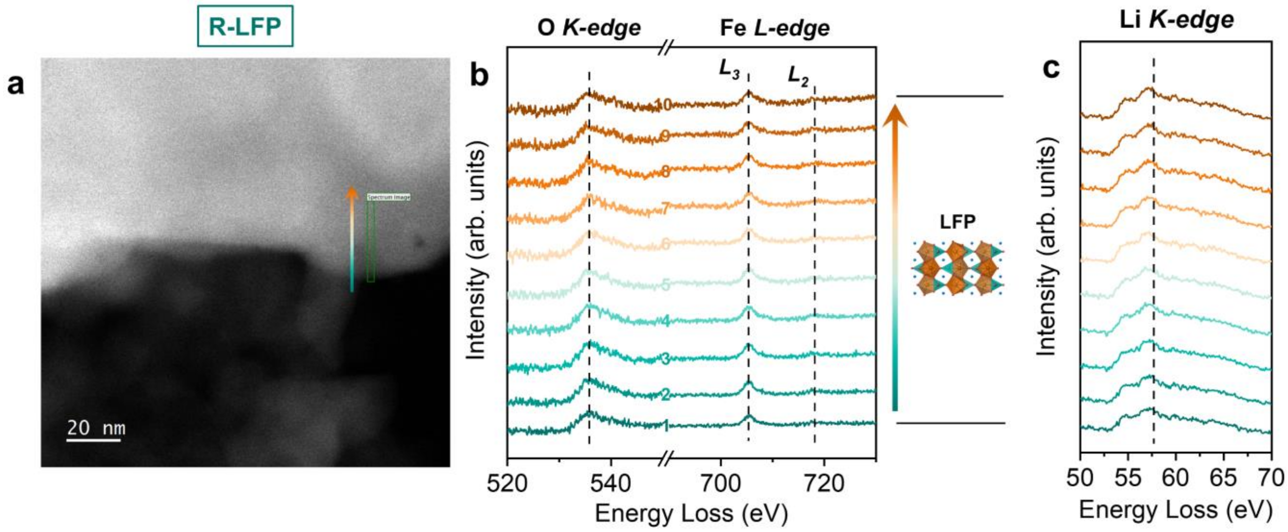


**Supplementary Fig. 26 a** STEM image, **b** O K-edge and Fe L-edge, and **c** Li K-edge EELS of R-LFP.

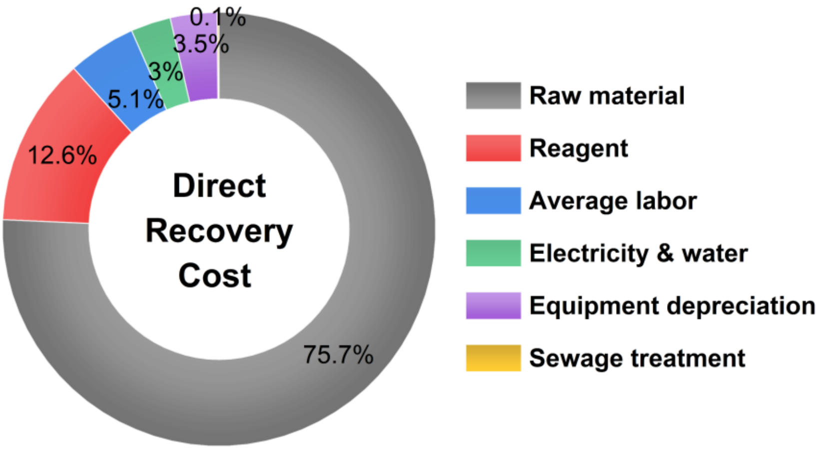


**Supplementary Fig. 27** Pie chart of the % costs involved in direct recovery.

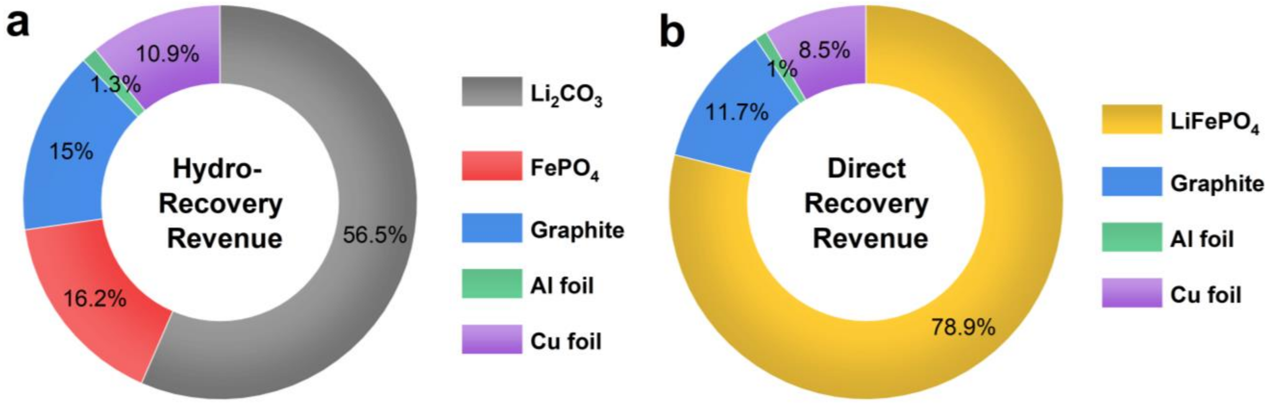


**Supplementary Fig. 28** Pie charts of the % revenues obtained using **a** hydro-recovery and **b** direct recovery.

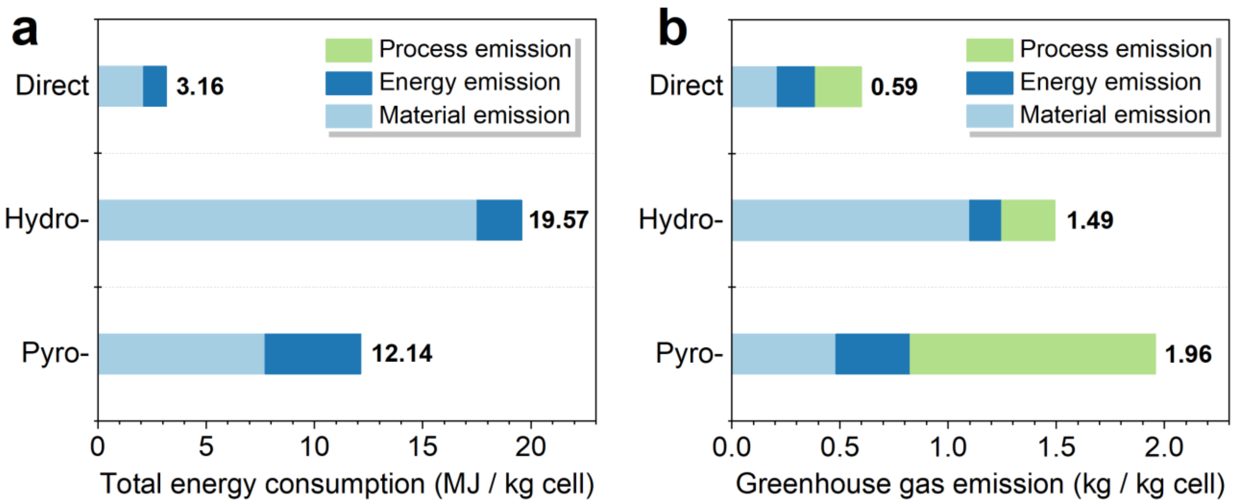


**Supplementary Fig. 29** **a** Total energy consumption and **b** GHG emissions of recycling 1 kg spent LFP batteries by pyro-, hydro-, and direct recovery.

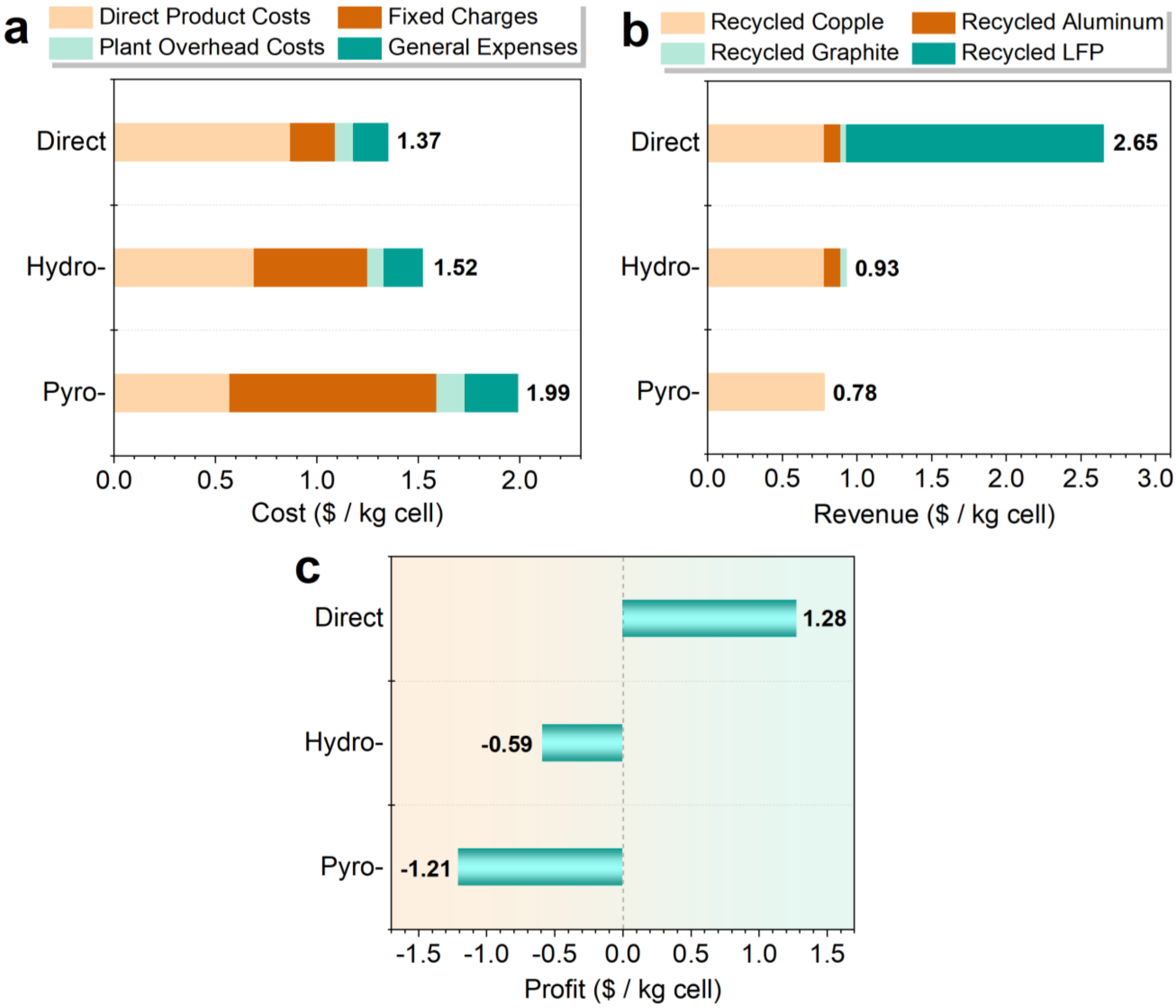


**Supplementary Fig. 30 a** Cost, **b** revenue, and **c** profit recycling 1 kg spent LFP batteries by pyro-, hydro-, and direct recovery.

The total costs of pyro-, hydro-, and direct recycling are \$1.99, \$1.52, and \$1.37 per kg of cells, respectively (**Supplementary Table 10 and Supplementary Fig. 30a**). Raw materials cost is mainly responsible for the manufacturing cost in direct recycling due to the high price of lithium salt. The recycled Al, Cu, graphite, and LFP is assumed to be sold to compensate some cost of the recycling processes (**Supplementary Table 11**). Notably, the recycled LFP is mainly attributed to the total revenue for direct recycling, which is higher than pyro- and hydro- recycling (**Supplementary Fig. 30b**). Therefore, the profits of pyro-, hydro-, and direct recycling are respectively \$-1.12, \$-0.59, and \$1.28 per kg of cells (**Supplementary Fig. 30c**).

**Supplementary Table 1** The degraded LIBs used in the recovery process and the corresponding basic parameters.

| | **LFP** | **NCM** | **LCO** |
|---|---|---|---|
| Type | Cyclinder cell | Pouch cell | Pouch cell |
| Manufacturer | LG (IFR18650) | Made in a laboratory | Sunwoda |
| Size | 18*65 mm | 80*55*3 mm | 95*45*4 mm |
| Weight | ~40 g | ~32 g | ~43 g |
| Voltage | 3.2 V | 3.7 V | 3.83 V |
| Capacity | 1.2 Ah | 1.7 Ah | 3.11 Ah |
| Profile Display |  |  |  |

**Supplementary Table 2** Element content and molar ratio of C-LFP, R-LFP and S-LFP samples based on ICP-OES results. (Note: C-LFP represents a commercial $LiFePO_4$ cathode)

| | Element content (wt%) | | | Molar ratio | |
|---|---|---|---|---|---|
| | **Li** | **P** | **Fe** | **Li/P** | **Li/Fe** |
| C-LFP | 4.44 | 18.48 | 33.27 | 1.07 | 1.07 |
| R-LFP-$Li_2$DHBN | 4.14 | 18.2 | 30.98 | 1.01 | 1.07 |
| R-LFP-$Li_2CO_3$ | 4.41 | 18.11 | 32.36 | 1.08 | 1.09 |
| R-LFP-LiOH | 4.46 | 18.41 | 32.14 | 1.08 | 1.11 |
| S-LFP | 3.84 | 18.5 | 32.26 | 0.92 | 0.98 |

**Supplementary Table 3** Summary of direct regeneration methods and their performance of LFP cathodes. (With annealing: No. 1-10; without annealing: No. 11-16; this work: No. 17)

| No. | Methods | Annealing conditions | Residual capacity (mAh/g) | Restored capacity (mAh/g) | Restored rate performance(mAh/g) | Ref. |
|---|---|---|---|---|---|---|
| 1 | Solid state sintering | 650 °C for 1 h | 140 at 0.2C, 125 at 1C | 147 at 0.2C, 130 at 1C | 100 at 5C, 80 at 10C | *4* |
| 2 | Solid state sintering | 700 °C for 3 h | 100 at 0.2C, 115 at 1C | 151 at 0.2C, 130 at 1C | 120 at 10C | *5* |
| 3 | Solid state sintering | 650 °C for 1 h | *Not provided.* | 135 at 0.2C, 130 at 1C | 108 at 5C | *6* |
| 4 | Solid state sintering | 700 °C for 8 h | *Not provided.* | 145 at 0.1C, 130 at 1C | 105 at 5C | *7* |
| 5 | Hydrothermal | 200 °C for 6 h | *Not provided.* | 136 at 0.1C, 105 at 1C | 84 at 2C | *8* |
| 6 | Hydrothermal | 700 °C for 6 h | 125 at 0.1C, 105 at 1C | 166 at 0.1C, 146 at 1C | 130 at 5C | *9* |
| 7 | Hydrothermal | 700 °C for 5 h | 101 at 1C | 139 at 1C | 108 at 5C, 100 at 10C | *10* |
| 8 | Solution relithiation | 600 °C for 2 h | 120 at 0.1C, 97 at 1C | 165 at 0.1C, 150 at 1C | 120 at 5C, 100 at 10C | *11* |
| 9 | Solution relithiation | 600 °C for 2 h | *Not provided.* | 166 at 0.1C, 150 at 1C | 135 at 5C | *12* |
| 10 | Molten Salt | 650 °C for 6 h | 120 at 1C | 130 at 1C | 110 at 5C | *13* |
| 11 | Graphite prelithiation | \ | 65 at 0.1C | 126 at 0.1C | 110 at 0.5C (full cells) | *14* |
| 12 | Chemical relithiation | \ | 160 at 0.5C | 160 at 0.5C | 110 at 5C, 95 at 10C | *15* |
| 13 | Separator prelithiation | \ | 110 at 0.1C | 160 at 0.1C, 150 at 1C | 140 at 2C (full cells) | *16* |
| 14 | One-step hydrothermal | \ | 125 at 0.1C, 100 at 1C | 146 at 0.2C, 141 at 1C | 128 at 5C | *17* |
| 15 | Electrochemical re-lithiation | \ | 125 at 0.2C | 137 at 0.2C, 134 at 1C | 108 at 5C | *18* |
| 16 | Electrically driven process | \ | *Not provided.* | 147 at 0.1C, 134 at 1C | 103 at 5C, 70 at 10C | *19* |
| 17 | Using organic lithium salt | 800 °C for 6 h | 102 at 0.1C, 98 at 1C | 157 at 0.1C, 140 at 1C | 111 at 5C, 97 at 10C | This work |

**Supplementary Table 4** Fitting result of equivalent circuit model for impedance parameters at different state of S-LFP sample. (OCV-open circuit voltage; C-charge; D-discharge)

| **SOC/DOD** | **$R_o$ (Ω)** | **$R_{ct}$ (Ω)** | **σ (Ω cm$^2$ s$^{-1/2}$)** |
|---|---|---|---|
| OCV | 1.167 | 47.78 | 33.43 |
| C-2.5V | 1.222 | 57.18 | 29.52 |
| C-3.4V | 1.207 | 52.67 | 42.42 |
| C-3.4V | 1.223 | 44.01 | 36.79 |
| C-3.5V | 1.126 | 38.52 | 45.26 |
| C-3.6V | 1.216 | 35.7 | 29.68 |
| C-4.0V | 1.23 | 32.92 | 18.67 |
| C-4.3V | 1.214 | 33.99 | 19.80 |
| D-4.0V | 1.205 | 36.48 | 21.35 |
| D-3.4V | 1.221 | 35.71 | 34.77 |
| D-3.3V | 1.232 | 44.05 | 42.25 |
| D-3.2V | 1.237 | 44.32 | 41.26 |
| D-3.0V | 1.25 | 43.01 | 45.18 |
| D-2.5V | 1.245 | 43.6 | 41.73 |

**Supplementary Table 5** Fitting result of equivalent circuit model for impedance parameters at different state of R-LFP-$Li_2$DHBN sample. (OCV-open circuit voltage; C-charge; D-discharge)

| SOC/DOD | $R_o$ (Ω) | $R_{ct}$ (Ω) | σ (Ω cm$^2$ s$^{-1/2}$) |
|---|---|---|---|
| OCV | 4.697 | 62.33 | 60.54 |
| C-2.5V | 4.363 | 72.34 | 63.63 |
| C-3.4V | 4.315 | 70.16 | 62.30 |
| C-3.4V | 4.215 | 60.28 | 58.66 |
| C-3.5V | 4.375 | 22.2 | 45.08 |
| C-3.6V | 4.234 | 21.49 | 66.73 |
| C-4.0V | 4.205 | 20.36 | 26.95 |
| C-4.3V | 4.203 | 20.11 | 27.69 |
| D-4.0V | 4.221 | 21.05 | 27.40 |
| D-3.4V | 4.208 | 20.53 | 12.64 |
| D-3.3V | 4.309 | 27.07 | 71.92 |
| D-3.2V | 4.325 | 27.61 | 70.38 |
| D-3.0V | 4.328 | 28.07 | 73.22 |
| D-2.5V | 4.287 | 27.81 | 82.19 |

**Supplementary Table 6** Structural parameters obtained from Rietveld refinement of the X-ray diffraction pattern of S-LFP. **Phase 1 $LiFePO_4$**: Space group: *Pnma*, $a$ = 10.32823 Å, $b$ = 6.00687 Å, $c$ = 4.69310 Å, $V$ = 291.161 Å$^3$, $\alpha = \beta = \gamma$ = 90°, Fraction: 78.70%. **Phase 2 $FePO_4$**: Space group: *Pnma*, $a$ = 5.79049 Å, $b$ = 9.81996 Å, $c$ = 4.78393 Å, $V$ = 272.025 Å$^3$, $\alpha = \beta = \gamma$ = 90°, Fraction: 21.30%.

| | **78.70% $LiFePO_4$** | | | | | **21.30% $FePO_4$** | | | | |
|---|---|---|---|---|---|---|---|---|---|---|
| **Atoms** | **Site** | **Wyckoff positions** | | | **Occupancy** | **Site** | **Wyckoff positions** | | | **Occupancy** |
| Li1 | 4a | 0 | 0 | 0 | 0.976 | NA | | | | |
| Fe2 | 4a | 0 | 0 | 0 | 0.024 | 4a | 0 | 0 | 0 | 0.002 |
| Fe1 | 4c | 0.28253 | 0.25000 | 0.97203 | 0.976 | 4c | 0.25000 | 0.27273 | 0.94955 | 0.998 |
| Li2 | 4c | 0.28253 | 0.25000 | 0.97203 | 0.024 | NA | | | | |
| P1 | 4c | 0.09772 | 0.25000 | 0.42512 | 1 | 4c | 0.25000 | 0.09681 | 0.40337 | 1 |
| O1 | 4c | 0.08747 | 0.25000 | 0.74366 | 1 | 4c | 0.25000 | 0.11319 | 0.69996 | 1 |
| O2 | 4c | 0.45553 | 0.25000 | 0.22315 | 1 | 4c | 0.25000 | 0.44344 | 0.17560 | 1 |
| O3 | 8d | 0.16361 | 0.04937 | 0.27832 | 1 | 8 | 0.04176 | 0.16562 | 0.25963 | 1 |

**Supplementary Table 7** Structural parameters obtained from Rietveld refinement of the X-ray diffraction pattern of R-LFP-$Li_2$DHBN. **Phase $LiFePO_4$**: Space group: *Pnma*, $a$ = 10.32347 Å, $b$ = 6.00249 Å, $c$ = 4.69709 Å, $V$ = 291.063 Å$^3$, $\alpha = \beta = \gamma$ = 90°, Fraction: 100(± 0.77)%.

| **Atoms** | **Site** | **Wyckoff positions** | | | **Occupancy** |
|---|---|---|---|---|---|
| Li1 | 4a | 0 | 0 | 0 | 0.988 |
| Fe2 | 4a | 0 | 0 | 0 | 0.012 |
| Fe1 | 4c | 0.28291 | 0.25000 | 0.97378 | 0.988 |
| Li2 | 4c | 0.28291 | 0.25000 | 0.97378 | 0.012 |
| P1 | 4c | 0.09857 | 0.25000 | 0.42966 | 1 |
| O1 | 4c | 0.08372 | 0.25000 | 0.73929 | 1 |
| O2 | 4c | 0.44779 | 0.25000 | 0.25914 | 1 |
| O3 | 8d | 0.15309 | 0.04042 | 0.26696 | 1 |

**Supplementary Table 8** Materials requirements (kg) to recycle 1 kg of spent batteries through different recycling technologies. (NR = Not Required)

| | **Pyro-** | **Hydro-** | **Direct** |
|---|---|---|---|
| Ammonium Hydroxide | NR | 0.031 | NR |
| Hydrochloric Acid | 0.21 | 0.012 | NR |
| Hydrogen Peroxide | 0.06 | 0.366 | NR |
| Sodium Hydroxide | NR | 0.561 | NR |
| Limestone | 0.30 | NR | NR |
| Sand | 0.15 | NR | NR |
| Sulfuric Acid | NR | 1.08 | NR |
| Soda Ash | NR | 0.02 | NR |
| Lithium Hydroxide | NR | NR | 0.047 |
| Citric Acid | NR | NR | NR |
| Lithium Carbonate | NR | NR | 0.030 |
| $Li_2$DHBN | NR | NR | 0.093 |

**Supplementary Table 9** Life-cycle environmental impacts of different recycling methods.

| | **Pyro-** | **Hydro-** | **Direct-** |
|---|---|---|---|
| **Total energy use in MJ per kg cell recycled** | | | |
| Total Energy | 12.140 | 19.570 | 3.165 |
| Fossil fuels | 11.098 | 18.075 | 2.638 |
| Coal | 3.521 | 3.106 | 1.055 |
| Natural gas | 6.662 | 13.406 | 0.528 |
| Petroleum | 0.915 | 1.564 | 1.483 |
| **Total Emissions in g per kg cell recycled** | | | |
| VOC | 0.129 | 0.211 | 0.059 |
| CO | 0.448 | 0.751 | 0.278 |
| $NO_x$ | 0.955 | 1.769 | 0.518 |
| PM10 | 0.100 | 0.146 | 0.078 |
| PM2.5 | 0.059 | 0.104 | 0.052 |
| $SO_x$ | 1.032 | 22.855 | 0.414 |
| BC | 0.017 | 0.023 | 0.014 |
| OC | 0.014 | 0.033 | 0.017 |
| $CH_4$ | 1.353 | 2.116 | 0.453 |
| $N_2O$ | 0.015 | 0.023 | 0.006 |
| $CO_2$ | 1,914 | 1,421 | 601 |
| $CO_2$ (w/ C in VOC & CO) | 1,915 | 1,423 | 598 |
| GHGs | 1,960 | 1,493 | 590 |

**Supplementary Table 10** Manufacturing cost details for different recycling processes per year (10,000 tons of spent batteries).

| | **Pyro-** | **Hydro-** | **Direct-** |
|---|---|---|---|
| **I. Manufacturing Cost, $/year** | $17,297,288 | $13,304,279 | $11,908,909 |
| A. Direct Product Costs | $5,711,445 | $6,855,798 | $8,751,139 |
| Raw Materials | $1,800,897 | $4,564,966 | $5,900,000 |
| Operating labor | $323,657 | $290,743 | $257,829 |
| Direct supervisory and clerical labor | $48,549 | $43,611 | $38,674 |
| Utilities | $492,828 | $225,111 | $588,017 |
| Maintenance and Repairs | $2,446,996 | $1,347,801 | $1,568,595 |
| Operating supplies | $367,049 | $202,170 | $235,289 |
| Laboratory charges | $32,366 | $29,074 | $25,783 |
| Patents and royalties | $199,103 | $152,321 | $136,951 |
| B. Fixed Charges | $10,176,242 | $5,607,403 | $2,225,221 |
| Depreciation | $4,784,468 | $2,633,067 | $168,938 |
| Local taxes | $1,957,597 | $1,078,241 | $954,876 |
| Insurance | $489,399 | $269,560 | $313,719 |
| Rent | $225,893 | $128,979 | $144,804 |
| Financing (interest) | $2,718,885 | $1,497,557 | $642,884 |
| C. Plant Overhead Costs | $1,409,601 | $841,078 | $932,549 |
| **II. General Expenses, $/year** | $2,613,013 | $1,927,858 | $1,786,230 |
| A. Administrative costs | $422,880 | $252,323 | $279,765 |
| B. Distribution and selling costs | $1,194,618 | $913,928 | $821,708 |
| C. R&D costs | $995,515 | $761,607 | $684,757 |
| **III. Total Product Cost, $/year** | $19,910,301 | $15,232,137 | $13,695,139 |

**Supplementary Table 11** Value of recycled materials ($/kg).

| | Pyro- | Hydro- | Direct- |
|---|---|---|---|
| Cu | $0.78 | $0.78 | $0.78 |
| Al | NA | $0.11 | $0.11 |
| Graphite | NA | $0.04 | $0.04 |
| $LiFePO_4$ | NA | NA | $4.82 |

# Original data of techno-economic analysis

**Supplementary Table 12** Basic data.

| The price of materials | | | | | |
|---|---|---|---|---|---|
| **No.** | **Item** | **Maket price** | **Unit** | **Update Date** | **Data Sources** |
| 1 | Degraded LFP batteries | 21700.00 | ¥ $t^{-1}$ | 16-May-22 | SMM |
| 2 | Degraded LFP powder | 65000.00 | ¥ $t^{-1}$ | 17-May-22 | SMM |
| 3 | LiOH | 475500.00 | ¥ $t^{-1}$ | 17-May-22 | SMM |
| 4 | $Li_2CO_3$ | 461500.00 | ¥ $t^{-1}$ | 18-May-22 | SMM |
| 5 | $Na_2CO_3$ | 3000.00 | ¥ $t^{-1}$ | 19-May-22 | 100PPI |
| 6 | $H_2SO_4$ | 2500.00 | ¥ $t^{-1}$ | 20-May-22 | 100PPI |
| 7 | $H_2O_2$ | 4200.00 | ¥ $t^{-1}$ | 21-May-22 | 100PPI |
| 8 | Ar | 2500.00 | ¥ $t^{-1}$ | 23-May-22 | 100PPI |
| 9 | Electricity | 0.72 | ¥ $Kw{\cdot}h^{-1}$ | 21-May-22 | BDB |
| 10 | Water | 3.20 | ¥ $t^{-1}$ | 22-May-22 | BDB |
| 11 | Average labor cost | 73000.00 | ¥ $a^{-1}$ | 28-May-22 | 51wctt |
| 12 | sewage treatment | 4.00 | ¥ $t^{-1}$ | 29-May-22 | 51wctt |
| 13 | $LiFePO_4$ cathode material | 155500.00 | ¥ $t^{-1}$ | 30-May-22 | SMM |
| ① 1 $ = 6.698 ￥ (Update time: 2022/7/5). ② Data Sources: SMM (https://www.smm.cn/), 100PPI (http://www.100ppi.com/ppi/), BDB (http://sz.bendibao.com/), 51wctt (https://mp.weixin.qq.com/s/AoXhIwQzLquIL_Csrkw7lw). | | | | | |

| Physical parameters | | | |
|---|---|---|---|
| **No.** | **Item** | **MW** | **Unit** |
| 1 | $LiFePO_4$ | 157.76 | g $mol^{-1}$ |
| 2 | $FePO_4$ | 150.82 | g $mol^{-2}$ |
| 3 | LiOH | 23.95 | g $mol^{-1}$ |
| 4 | $Li_2CO_3$ | 73.89 | g $mol^{-1}$ |
| 5 | $Li_2$DHBN | 146.88 | g $mol^{-1}$ |
| 7 | $H_2SO_4$ | 98.08 | g $mol^{-1}$ |
| 8 | $H_2O_2$ | 34.01 | g $mol^{-1}$ |
| 9 | $Na_2CO_3$ | 105.99 | g $mol^{-2}$ |
| 10 | Li | 6.94 | g $mol^{-1}$ |
| 11 | Fe | 55.85 | g $mol^{-1}$ |
| 12 | P | 30.97 | g $mol^{-1}$ |
| 13 | O | 16.00 | g $mol^{-1}$ |
| 14 | C | 12.01 | g $mol^{-1}$ |
| 15 | H | 1.00 | g $mol^{-1}$ |
| 16 | N | 14.00 | g $mol^{-2}$ |
| 17 | Na | 22.99 | g $mol^{-1}$ |

| Compenent in a LFP battery | | | |
|---|---|---|---|
| **No.** | **Item** | **Proportion** | **Unit** |
| 1 | Cathode active material | 25.00 | % |
| 2 | Anode active material | 13.00 | % |
| 3 | Al foil | 6.00 | % |
| 4 | Cu foil | 10.00 | % |
| 5 | Separator | 3.00 | % |
| 6 | Electrolyte | 16.00 | % |
| 7 | Shell | 27.00 | % |
| Ref: https://doi.org/10.1016/j.est.2020.102217 | | | |

**Supplementary Table 13** Hydro- recovery cost analysis.

| Cost analysis based on Hydro- recovery | | | | | | | |
|---|---|---|---|---|---|---|---|
| **Main** | **No.** | **Item** | **Unit Price (¥ $t^{-1}$)** | **Dose (t)** | **Note** | **Data Source** | **Cost (¥)** |
| Raw material | 1 | Degraded battery | 21700.00 | 1.0000 | **250 kg of the degraded LFP can be sorted from per 1 ton of degraded battery.** | https://doi.org/10.1016/j.est.2020.102217 | 21700.00 |
| | 2 | Degraded LFP | | 0.0000 | | | 0.00 |
| | subtotal (¥) | | | | | | 21700.00 |
| **Main** | **No.** | **Item** | **Unit Price (¥ $t^{-1}$)** | **Dose (t)** | **Note** | **Data Source** | **Cost (¥)** |
| Reagent | 3 | $H_2SO_4$ | 2500.00 | 0.0886 | **Used as the leaching agent to extraction lithium.** | DOI: 10.1021/acssuschemeng.7b01594 | 221.48 |
| | 4 | $H_2O_2$ | 4200.00 | 0.1116 | **Used as the oxidization to extraction lithium.** | | 468.56 |
| | 5 | $Na_2CO_3$ | 3000.00 | 0.0541 | **Used to precipitate lithium.** | | 162.23 |
| | subtotal (¥) | | | | | | 852.28 |
| **Main** | **No.** | **Item** | **Unit Price (¥ $a^{-1}$)** | **Dose (a)** | **Note** | **Data Source** | **Cost (¥)** |
| Average labor | 6 | Degraded battery disassembly | 73000.00 | 0.01 | | https://doi.org/10.1016/j.xcrp.2022.100741 | 730.00 |
| | 7 | Material preparation | 73000.00 | 0.02 | | | 1460.00 |
| | subtotal (¥) | | | | | | 2190.00 |
| **Main** | **No.** | **Item** | **Unit Price(¥ $t^{-1}$ & ¥ $kwh^{-1}$)** | **Dose (t & Kwh)** | **Note** | **Data Source** | **Cost (¥)** |
| Electricity & water | 8 | Water | 3.20 | 500.00 | | https://doi.org/10.1016/j.xcrp.2022.100741 | 1600.00 |
| | 9 | Electricity | 0.72 | 500.00 | | | 360.00 |
| | subtotal (¥) | | | | | | 1960.00 |
| **Main** | **No.** | **Item** | **Unit Price (¥ $t^{-1}$)** | **Dose (t)** | **Note** | **Data Source** | **Cost (¥)** |
| Equipment depreciation | 10 | Equipment depreciation | 5000.00 | 0.50 | | DOI:10.3969/j.issn.1009-847X.2018.10.006 | 2500.00 |
| | subtotal (¥) | | | | | | 2500.00 |
| **Main** | **No.** | **Item** | **Unit Price (¥ $t^{-1}$)** | **Dose (t)** | **Note** | **Data Source** | **Cost (¥)** |
| Sewage treatment | 11 | Sewage treatment | 40.00 | 20.00 | | DOI:10.3969/j.issn.1009-847X.2018.10.006 | 800.00 |
| | subtotal (¥) | | | | | | 800.00 |
| **Total Cost (¥)** | | | | | | | **30002.28** |

① In Supplementary Table 13, we calculated the cost per one ton of recycled cathode materials. The recycle process can be divided into three steps: disassembly of degraded battery, seperation of cathode active material, extraction of lithium.

② We assume that the failure degree of spent LFP batterry is consistent ($Li_{0.8}FePO_4$) based on Hydro- and direct recovery.

**Supplementary Table 14** Direct recovery cost analysis.

| Cost analysis based on Direct recovery | | | | | | | |
|---|---|---|---|---|---|---|---|
| **Main** | **No.** | **Item** | **Unit Price (¥ $t^{-1}$)** | **Dose (t)** | **Note** | **Data Source** | **Cost (¥)** |
| Raw material | 1 | Degraded battery | 21700.00 | 1.0000 | **250 kg of the degraded LFP can be sorted from per 1 ton of degraded battery.** | https://doi.org/10.1016/j.est.2020.102217 | 21700.00 |
| | 2 | Degraded LFP | 0.00 | 0.0000 | | | 0.00 |
| | subtotal (¥) | | | | | | 21700.00 |
| **Main** | **No.** | **Item** | **Unit Price (¥ $t^{-1}$)** | **Dose (t)** | **Note** | **Data Source** | **Cost (¥)** |
| Reagent | 3 | $Li_2CO_3$ | 461500.00 | 0.0117 | **Used as the lithium salt to restore the degraded LFP.** | SMM | 5403.82 |
| | 4 | LiOH | 475500.00 | 0.0076 | **Used as the lithium salt to restore the degraded LFP.** | | 3609.35 |
| | 5 | $Li_2DHBN$ | 199780.00 | 0.0233 | **Used as the lithium salt to restore the degraded LFP.** | | 4650.05 |
| | 6 | Ar | 2500.00 | 0.01 | **Used as the protective atmospherer during regeneraiton process.** | | 25.00 |
| | subtotal (¥) | | | | | | 4650.05 |
| **Main** | **No.** | **Item** | **Unit Price (¥ $a^{-1}$)** | **Dose (a)** | **Note** | **Data Source** | **Cost (¥)** |
| Average labor | 7 | Disassemble degraded battery | 73000.00 | 0.01 | | https://doi.org/10.1016/j.xcrp.2022.100741 | 730.00 |
| | 8 | Material preparation | 73000.00 | 0.01 | | | 730.00 |
| | subtotal (¥) | | | | | | 1460.00 |
| **Main** | **No.** | **Item** | **Unit Price(¥ $t^{-1}$ & ¥ $kwh^{-1}$)** | **Dose (t & Kwh)** | **Note** | **Data Source** | **Cost (¥)** |
| Electricity & water | 9 | Water | 3.20 | 200.00 | | https://doi.org/10.1016/j.xcrp.2022.100741 | 640.00 |
| | 10 | Electricity | 0.72 | 300.00 | | | 216.00 |
| | subtotal (¥) | | | | | | 856.00 |
| **Main** | **No.** | **Item** | **Unit Price (¥ $t^{-1}$)** | **Dose (t)** | **Note** | **Data Source** | **Cost (¥)** |
| Equipment depreciation | 11 | Equipment depreciation | 5000.00 | 0.20 | | DOI:10.3969/j.issn.1009-847X.2018.10.006 | 1000.00 |
| | subtotal (¥) | | | | | | 1000.00 |
| **Main** | **No.** | **Item** | **Unit Price (¥ $t^{-1}$)** | **Dose (t)** | **Note** | **Data Source** | **Cost (¥)** |
| Sewage treatment | 12 | Sewage treatment | 40.00 | 1.00 | | DOI:10.3969/j.issn.1009-847X.2018.10.006 | 40.00 |
| | subtotal (¥) | | | | | | 40.00 |
| **Total Cost (¥)** | | | | | | | **29706.05** |

① In Supplementary Table 14, we calculated the cost per one ton of recycled cathode materials. The recycle process can be divided into three steps: disassembly of degraded battery, seperation of cathode active material, regeneration of LFP material.

② We assume that the failure degree of spent LFP batterry is consistent ($Li_{0.8}FePO_4$) based on Hydro- and direct recovery.

| Different Li content in degraded LFP ($Li_xFePO_4$) | | | |
|---|---|---|---|
| 0.80 | | Cost (¥) | Total Cost (¥) |
| **The consumption of $Li_2CO_3$ (t)** | 0.0117 | 5403.82 | 30459.82 |
| **The consumption of LiOH (t)** | 0.0076 | 3609.35 | 28665.35 |
| **The consumption of $Li_2$DHBN (t)** | 0.0233 | 4650.05 | 29706.05 |
| Note: We assume that different residual Li content determines the consumption of lithium salt in regeneration process. | | | |

| Cost analysis of 1 ton $Li_2$DHBN | | | | |
|---|---|---|---|---|
| **Raw materials** | **Unit Price (¥ $t^{-1}$)** | **Dose (t)** | **Data Source** | **Cost (¥)** |
| 3,4-dihydroxybenzonitrile | 100000.00 | 0.919 | https://b2b.baidu.com/ | 91900.00 |
| tetrahydrofuran (THF) | 8000.00 | 12.000 | | 96000.00 |
| lithium hydride (LiH) | 110000.00 | 0.108 | | 11880.00 |
| subtotal (¥) | 199780.00 | | | |

**Supplementary Table 15** Hydro- recovery revenue analysis.

| Revenue analysis based on Hydro- recovery | | | | | | | | |
|---|---|---|---|---|---|---|---|---|
| **No.** | **Item** | **Material** | **Recovery yield (%)** | **Production (t)** | **Market price (￥ $t^{-1}$)** | **Revenue (￥)** | **Update Date** | **Data Sources** |
| 1 | **Lithium salt** | $Li_2CO_3$ | 95 | 0.0445 | 461,500.00 | 20534.50 | 16-May-22 | SMM |
| 2 | **Precursor** | $FePO_4$ | 95 | 0.2271 | 26,000.00 | 5903.36 | 16-May-22 | SMM |
| 3 | **Anode material** | Graphite | 98 | 0.1274 | 42,900.00 | 5465.46 | 16-May-22 | SMM |
| 4 | **Curret collector** | Al foil | 90 | 0.0540 | 8,671.00 | 468.23 | 16-May-22 | https://doi.org/10.1016/j.joule.2020.10.008 |
| 5 | **Curret collector** | Cu foil | 90 | 0.0900 | 44,022.00 | 3961.98 | 16-May-22 | https://doi.org/10.1016/j.joule.2020.10.009 |
| 6 | **Separator** | | 98 | 0.0294 | NA | NA | | |
| 7 | **Electrolyte** | | 90 | 0.1440 | NA | NA | | |
| 8 | **Shell** | | 98 | 0.1568 | NA | NA | | |
| subtotal (￥) 32314.9741 | | | | | | | | |

Note: ① We assume that the failure degree of spent LFP batterry is consistent ($Li_{0.8}FePO_4$) based on Hydro- and direct recovery. ② The proportion of each compenent is 27% of cathode material, 13% of graphite, 6% of Al foil, 10% of Cu foil, 3% of separator, 16% of electrolyte, and 27% of shell (Ref: https://doi.org/10.1016/j.est.2020.102217). ③ The value of $Li_2CO_3$, $FePO_4$, and graphite is calculated based on the real market price from SMM. ④ The value of separator, electrolyte and shell is hard to assess in real process, therefore, these components are not included in our revenue analysis.

| **Different Li content in degraded LFP ($Li_xFePO_4$)** | | |
|---|---|---|
| 0.80 | | **Revenue (￥)** |
| **The production of $Li_2CO_3$ (t)** | 0.0445 | 20534.50 |

Note: We assume that different residual Li content determines the production of lithium salt in Hydro- recovery process.

**Supplementary Table 16** Direct recovery revenue analysis.

| Revenue analysis based on Direct recovery | | | | | | | | |
|---|---|---|---|---|---|---|---|---|
| **No.** | **Item** | **Material** | **Recovery yield (%)** | **Production (t)** | **Market price (￥ $t^{-1}$)** | **Revenue (￥)** | **Update Date** | **Data Sources** |
| 1 | **Cathode Material** | $LiFePO_4$ | 95 | 0.2375 | 155,500.00 | 36931.25 | 16-May-22 | SMM |
| 2 | **Anode material** | Graphite | 98 | 0.1274 | 42,900.00 | 5465.46 | 16-May-22 | SMM |
| 3 | **Curret collector** | Al foil | 90 | 0.0540 | 8,671.00 | 468.23 | 16-May-22 | https://doi.org/10.1016/j.joule.2020.10.009 |
| 4 | **Curret collector** | Cu foil | 90 | 0.0900 | 44,022.00 | 3961.98 | 16-May-22 | https://doi.org/10.1016/j.joule.2020.10.009 |
| 5 | **Separator** | | 95 | 0.0285 | NA | NA | | |
| 6 | **Electrolyte** | | 90 | 0.1440 | NA | NA | | |
| 7 | **Shell** | | 98 | 0.2646 | NA | NA | | |
| subtotal (￥) 41213.3740 | | | | | | | | |
| Note: ① We assume that the failure degree of spent LFP batterry is consistent ($Li_{0.8}FePO_4$) based on Hydro- and direct recovery. ② The proportion of each compenent is 27% of cathode material, 13% of graphite, 6% of Al foil, 10% of Cu foil, 3% of separator, 16% of electrolyte, and 27% of shell (Ref: https://doi.org/10.1016/j.est.2020.102217). ③ The value of regenerated $LiFePO_4$ is calculated based on the real market price from SMM. ④The value of separator, electrolyte and shell is hard to assess in real process, therefore, these compenents are not included in our revenue analysis. | | | | | | | | |

**Supplementary Table 17** Hydro- recovery cost results.

| Hydro- & Direct recovery cost results | | | | | | | | | | | | | | | |
|---|---|---|---|---|---|---|---|---|---|---|---|---|---|---|---|
| No. | Li Content | Hydro- recovery cost（¥） | | | | | | | Direct recovery cost（¥） | | | | | | |
| | | Raw material | Reagent | Average labor | Electricity & water | Equipment depreciation | Sewage treatment | Total cost | Raw material | Reagent | Average labor | Electricity & water | Equipment depreciation | Sewage treatment | Total cost |
| 1 | 0.80 | 21700.00 | 852.28 | 2190.00 | 1960.00 | 2500.00 | 800.00 | 30002.28 | 21700.00 | 4650.05 | 1460.00 | 856.00 | 1000.00 | 40.00 | 29706.05 |
| 2 | 0.60 | 21700.00 | 852.28 | 2190.00 | 1960.00 | 2500.00 | 800.00 | 30002.28 | 21700.00 | 9300.10 | 1460.00 | 856.00 | 1000.00 | 40.00 | 34356.10 |
| 3 | 0.40 | 21700.00 | 852.28 | 2190.00 | 1960.00 | 2500.00 | 800.00 | 30002.28 | 21700.00 | 13950.16 | 1460.00 | 856.00 | 1000.00 | 40.00 | 39006.16 |
| 4 | 0.20 | 21700.00 | 852.28 | 2190.00 | 1960.00 | 2500.00 | 800.00 | 30002.28 | 21700.00 | 18600.21 | 1460.00 | 856.00 | 1000.00 | 40.00 | 43656.21 |

**Supplementary Table 18** Direct recovery cost results.

| Hydro- & Direct recovery revenue results | | | | | | | | | | | | |
|---|---|---|---|---|---|---|---|---|---|---|---|---|
| No. | Li Content | Hydro- recovery revenue (¥) | | | | | | Direct recovery revenue（¥） | | | | |
| | | $Li_2CO_3$ | $FePO_4$ | Graphite | Al foil | Cu foil | Total revenue | $LiFePO_4$ | Graphite | Al foil | Cu foil | Total revenue |
| 1 | 0.80 | 20534.50 | 5903.36 | 5465.46 | 468.23 | 3961.98 | 36333.53 | 36931.25 | 5465.46 | 468.23 | 3961.98 | 46826.92 |
| 2 | 0.60 | 15400.87 | 5903.36 | 5465.46 | 468.23 | 3961.98 | 31199.90 | 36931.25 | 5465.46 | 468.23 | 3961.98 | 46826.92 |
| 3 | 0.40 | 10267.25 | 5903.36 | 5465.46 | 468.23 | 3961.98 | 26066.28 | 36931.25 | 5465.46 | 468.23 | 3961.98 | 46826.92 |
| 4 | 0.20 | 5133.62 | 5903.36 | 5465.46 | 468.23 | 3961.98 | 20932.65 | 36931.25 | 5465.46 | 468.23 | 3961.98 | 46826.92 |

**Supplementary Table 19** Profit calculation.

| Recovery profit results | | | |
|---|---|---|---|
| **No.** | **Li Content** | **Hydro- profit (￥)** | **Direct profit (￥)** |
| 1 | 0.80 | 6331.25 | 17120.87 |
| 2 | 0.60 | 1197.62 | 12470.82 |
| 3 | 0.40 | -3936.00 | 7820.76 |
| 4 | 0.20 | -9069.63 | 3170.71 |

**Supplementary References**

1. Hong, L., *et al.* Two-dimensional lithium diffusion behavior and probable hybrid phase transformation kinetics in olivine lithium iron phosphate. *Nat. Commun.* **8**, 1194 (2017).

2. Gu, W., *et al.* Recyclable, self-healing solid polymer electrolytes by soy protein-based dynamic network. *Adv. Sci.* **9**, 2103623 (2022).

3. Shen, Z., Cao, L., Rahn, C. D. & Wang, C. Y. Least squares galvanostatic intermittent titration technique (LS-GITT) for accurate solid phase diffusivity measurement. *J. Electrochem. Soc.* **160**, A1842-A1846 (2013).

4. Li, X. L., Zhang, J., Song, D. W., Song, J. S. & Zhang, L. Q. Direct regeneration of recycled cathode material mixture from scrapped $LiFePO_4$ batteries. *J. Power Sources* **345**, 78-84 (2017).

5. Li, J., Wang, Y., Wang, L. H., Liu, B. & Zhou, H. M. A facile recycling and regeneration process for spent $LiFePO_4$ batteries. *J. Mater. Sci.: Mater. Electron.* **30**, 14580-14588 (2019).

6. Chen, J. P., Li, Q. W., Song, J. S., Song, D. W., Zhang, L. Q. & Shi, X. X. Environmentally friendly recycling and effective repairing of cathode powders from spent $LiFePO_4$ batteries. *Green Chem.* **18**, 2500-2506 (2016).

7. Song, X., *et al.* Direct regeneration of cathode materials from spent lithium iron phosphate batteries using a solid phase sintering method. *RSC Adv.* **7**, 4783-4790 (2017).

8. Song, Y. F., *et al.* Regeneration of $LiFePO_4$ from spent lithium-ion batteries via a facile process featuring acid leaching and hydrothermal synthesis. *Green Chem.* **23**, 3963-3971 (2021).

9. Chen, B. B., *et al.* Direct regeneration and performance of spent $LiFePO_4$ via a green efficient hydrothermal technique. *J. Alloys Compd.* **924**, 166487 (2022).

10. Jia, K., *et al.* Long-life regenerated $LiFePO_4$ from spent cathode by elevating the *d*-band center of Fe. *Adv. Mater.*, e2208034 (2022). Preprint at https://doi.org/10.1002/adma.202208034

11. Xu, P. P., *et al.* Efficient direct recycling of lithium-ion battery cathodes by targeted healing. *Joule* **4**, 2609-2626 (2020).

12. Fan, M., *et al.* Structural restoration of degraded $LiFePO_4$ cathode with enhanced kinetics using residual lithium in spent graphite anodes. *CCC Chem.*, 1-13 (2022). Preprint at https://doi.org/10.31635/ccschem.022.202201996

13. Liu, X., Wang, M. M., Deng, L. P., Cheng, Y. J., Gao, J. & Xia, Y. G. Direct regeneration of spent

lithium iron phosphate via a low-temperature molten salt process coupled with a reductive environment. *Ind. Eng. Chem. Res.* **61**, 3831-3839 (2022).

14. Wang, T., *et al.* Direct regeneration of spent $LiFePO_4$ via a graphite prelithiation strategy. *Chem. Commun.* **56**, 245-248 (2019).

15. Wu, C., *et al.* Direct regeneration of spent Li-ion battery cathodes via chemical relithiation reaction. *ACS Sustain. Chem. Eng.* **9**, 16384-16393 (2021).

16. Fan, M., *et al.* In situ electrochemical regeneration of degraded $LiFePO_4$ electrode with functionalized prelithiation separator. *Adv. Energy Mater.* **12**, 2103630 (2022).

17. Jing, Q. K., Zhang, J. L., Liu, Y. B., Zhang, W. J., Chen, Y. Q. & Wang, C. Y. Direct regeneration of spent $LiFePO_4$ cathode material by a green and efficient one-step hydrothermal method. *ACS Sustain. Chem. Eng.* **8**, 17622-17628 (2020).

18. Zhou, S. Y., *et al.* Direct recovery of scrapped $LiFePO_4$ by a green and low-cost electrochemical re-lithiation method. *Green Chem.* **24**, 6278-6286 (2022).

19. Peng, D., *et al.* Efficient regeneration of retired $LiFePO_4$ cathode by combining spontaneous and electrically driven processes. *Green Chem.* **24**, 4544-4556 (2022).